The Journal of Chemical Physics

Hybrid theoretical models for molecular nanoplasmonics

Cite as: J. Chem. Phys. **153**, 200901 (2020); https://doi.org/10.1063/5.0027935
Submitted: 01 September 2020 . Accepted: 29 October 2020 . Published Online: 24 November 2020

E. Coccia, J. Fregoni, C. A. Guido, M. Marsili, S. Pipolo, and S. Corni

The Journal of Chemical Physics PERSPECTIVE scitation.org/journal/jcp

Hybrid theoretical models for molecular nanoplasmonics

Cite as: J. Chem. Phys. 153, 200901 (2020); doi: 10.1063/5.0027935
Submitted: 1 September 2020 • Accepted: 29 October 2020 •
Published Online: 24 November 2020

E. Coccia,[1,a)] J. Fregoni,[2,3] C. A. Guido,[4] M. Marsili,[4] S. Pipolo,[5] and S. Corni[3,4,a)]

AFFILIATIONS

[1]Dipartimento di Scienze Chimiche e Farmaceutiche, Università di Trieste, via L. Giorgieri 1, 34127 Trieste, Italy
[2]Dipartimento di Scienze Fisiche, Informatiche e Matematiche, Università di Modena e Reggio Emilia, via Campi 213/A, 41125 Modena, Italy
[3]Istituto Nanoscienze-CNR, via Campi 213/A, 41125 Modena, Italy
[4]Dipartimento di Scienze Chimiche, Università di Padova, via F. Marzolo 1, 35131 Padova, Italy
[5]Université de Lille, CNRS, Centrale Lille, ENSCL, Université d'Artois UMR 8181—UCCS Unité de Catalyse et Chimie du Solide, F-59000 Lille, France

[a)]**Authors to whom correspondence should be addressed:** ecoccia@units.it and stefano.corni@unipd.it

ABSTRACT

The multidisciplinary nature of the research in molecular nanoplasmonics, i.e., the use of plasmonic nanostructures to enhance, control, or suppress properties of molecules interacting with light, led to contributions from different theory communities over the years, with the aim of understanding, interpreting, and predicting the physical and chemical phenomena occurring at molecular- and nano-scale in the presence of light. Multiscale hybrid techniques, using a different level of description for the molecule and the plasmonic nanosystems, permit a reliable representation of the atomistic details and of collective features, such as plasmons, in such complex systems. Here, we focus on a selected set of topics of current interest in molecular plasmonics (control of electronic excitations in light-harvesting systems, polaritonic chemistry, hot-carrier generation, and plasmon-enhanced catalysis). We discuss how their description may benefit from a hybrid modeling approach and what are the main challenges for the application of such models. In doing so, we also provide an introduction to such models and to the selected topics, as well as general discussions on their theoretical descriptions.

I. INTRODUCTION

The interaction between light and composite systems at nanoscale ignited over the years the interest of different scientific communities,[1–7] attracted by the multidisciplinary nature of the topic and by the simultaneous fundamental and technological implications associated with this research field.

The individual components of these systems can be single molecules and nanostructures, possibly aggregated in nano- or even mesoscopic assemblies. As a result of the mutual interaction between the various elements of the system, chemical and physical properties of the composite system can largely differ from those of the single components, and the light-induced response can strongly deviate from the sum of the responses of each constituent.

More specifically, one class of phenomena, which has been extensively studied and, at the same time, is still characterized by a number of open questions, is that related to the molecular nanoplasmonics.[8] Namely, molecular nanoplasmonics investigates how plasmon-induced processes modify the properties of a molecular system close to a metal nanoparticle (NP).

NP plasmon effects are used to strongly modify the spectroscopic signal of molecules interacting with it.[9,10] Outcomes of plasmon-enhanced spectroscopy then depend on the shape and nature of the NP, on the geometric configuration of the NP + molecule(s) system,[8,11,12] and on the type of the applied external pulse.[13] Examples of plasmon-based experimental techniques and phenomena are surface enhanced Raman spectroscopy (SERS),[14,15] in which the molecular Raman signal is enhanced by several orders

of magnitude; plasmon-modified (enhanced or quenched, according to the relative molecular orientation with respect to the NP) molecular fluorescence;[16,17] photochemical reactions, which can be altered by plasmon-assisted mechanisms,[5,18] as hot-carrier (HC) generation and transfer from the NP to the molecule,[4] and the strong coupling in plasmonic nanocavities containing the molecule, which leads to hybrid light–matter states.[19,20]

The theoretical modeling of systems of such an intrinsic complexity requires a multiscale description, which is able to capture the individual and collective behavior of the composite system. Focusing on the molecular nanoplasmonics,[8,21–28] the requirement of a multiscale hybrid approach arises naturally: the small subsystem, i.e., the single molecule or the molecular aggregate, and the larger component, i.e., the nanostructure, need to be described by means of different approaches. The level of description is adapted according to the different size and level of accuracy required/affordable. Hybrid methods for molecular plasmonics can be categorized based on the level of theory for the molecular target and on the description of the plasmonic nanostructure. Considering the molecular target, we can distinguish three main categories, ordered in terms of increasing complexity: (i) classical polarizable point dipole models ("dip" in the rest of this work),[22,29–34] where the molecule is characterized only by using a frequency-dependent polarizability tensor (often isotropic); (ii) two-level quantum mechanical models ("2lev" from now on), a model derived from quantum optics where the molecule is described as a quantum system with two states (ground and excited),[7] separated by a certain excitation energy and coupled through a transition dipole, possibly obtained from empirical data; (iii) fully atomistic models based on a quantum-chemistry description ("QM," to comply with the standard acronyms of hybrid quantum-chemistry models),[2,6,11,12,24–28,35–46] providing chemical details and predictive power. The present classification is somewhat rough, and, in particular, for polaritonic chemistry, the 2lev model has been extended to include the dependence on one or a few nuclear coordinates to model photochemistry.[47]

The NP can be seen as an effective environment interacting with and responding to the external electromagnetic field and the molecular probe. An accurate representation of the NP, in terms of atomic and electronic structure and dynamics, is often not necessary, and modeling the NP response, as a whole, by using classical methods is indeed a reliable approach.[2,6,35] When combined with the QM description of the molecule, such hybrid approaches are called QM/classical. A full QM description of the nanosystem is limited by the computationally accessible size of the system (a few nanometers), and perhaps, it is also not needed in many cases, judging from the good quality of the classical electromagnetic descriptions of the optical properties of metal NPs.[48–50] Such hybrid approaches permit us to successfully study plasmon-induced phenomena involving molecules, such as plasmon-spectroscopy (SERS and fluorescence) and plasmon-modified chemical reactions.

QM/classical approaches can be further classified by following the modeling of the NP:[6] QM/continuum, in which the NP is defined as a continuum characterized by a dielectric function,[11,12,27,36,38–42,45,46] and QM/discrete, in which a discrete, atomistic but classical description of the NP is adopted.[24–26,28,37,43,44]

QM/continuum models can be seen as an extension of continuum solvation models, which were proposed in the literature over the years, such as the polarizable continuum model (PCM).[51,52] The NP is, in fact, treated as a finite dielectric medium, with a given size, shape, and nature, and it is characterized by a frequency-dependent permittivity function $\epsilon(\omega)$. The ϵ function describes the NP electromagnetic response to the external field and is generated by the electronic density of the molecule close to the NP. QM/continuum approaches were originally defined in the frequency domain, i.e., considering monochromatic external perturbations, usually coupled to a density functional theory (DFT) and a time-dependent DFT (TDDFT) description of the molecule.[11,21,36] Recent developments extended the QM/continuum models to the time domain,[13,53] allowing one to directly simulate time-resolved (plasmon-enhanced) spectroscopies.

Analogously, QM/discrete approaches can be seen as an extension of QM/MM approaches to molecular plasmonics.[6] Here, a proper description of the response of the NP atoms to an external electromagnetic field has been developed in terms of atomic polarizabilities and capacitances (the discrete interaction model of Jensen and co-workers[37,54] and the model by Rinkevicius *et al.*[43]) and by a discretized version of the Drude model, as in the ωFQ approach.[55,56]

In addition to the QM molecule and the NP, other components of the systems may also require to be modeled. For example, a solvent that embeds both the molecule and the NP is often included as an additional dielectric in QM/continuum models (QM/discrete models have mostly been applied to a solvent-free environment). The complexity of some molecules, such as light-harvesting complexes in proteins, has prompted the extension of QM/continuum models to a three-layer description:[6] QM for the protein chromophores, classical atomistic molecular mechanics for the protein scaffold, and a continuum description for the NP and the surrounding solvent.[57–59]

QM/classical models have been originally devised for (and so far mostly applied to) spectroscopy, such as SERS[54,60,61] (and its non-linear extension surface enhanced hyper Raman scattering),[25] plasmon-modified molecular fluorescence,[11,62] Surface Enhanced Infrared Absorption (SEIRA),[63] excitation energy transfer,[64] and surface enhanced two-photon absorption.[65] Moreover, all these phenomena have been investigated within a traditional quantum-chemistry picture, considering response theory in the frequency domain and neglecting decoherence effects. Based on this *status quo*, we decided to focus this Perspective on a few subtopics of molecular plasmonics—different from spectroscopies—that are rapidly developing and of broad interest and that also represent active fields of research of our group. We shall, in particular, discuss the potential usefulness of QM/continuum models to treat such topics, the status of their application, and the theoretical challenges to be overcome for their practical applications. Moreover, we shall also review recent developments in QM/continuum modeling that allows us to embrace a natively time-dependent picture of molecular nanoplasmonics,[53] including quantum decoherence effects.[13] Such a picture is, in fact, one of the ingredients to tackle some of the forefront molecular nanoplasmonics subtopics just mentioned.

More in detail, the following discussion will focus on (Fig. 1): the interplay between the plasmonic and decoherence effects on the optical properties of molecules[13,66] and light-harvesting complexes,[58,59] the strong-coupling regime between light and matter for molecules in plasmonic nanocavities[19,67] and its relation with

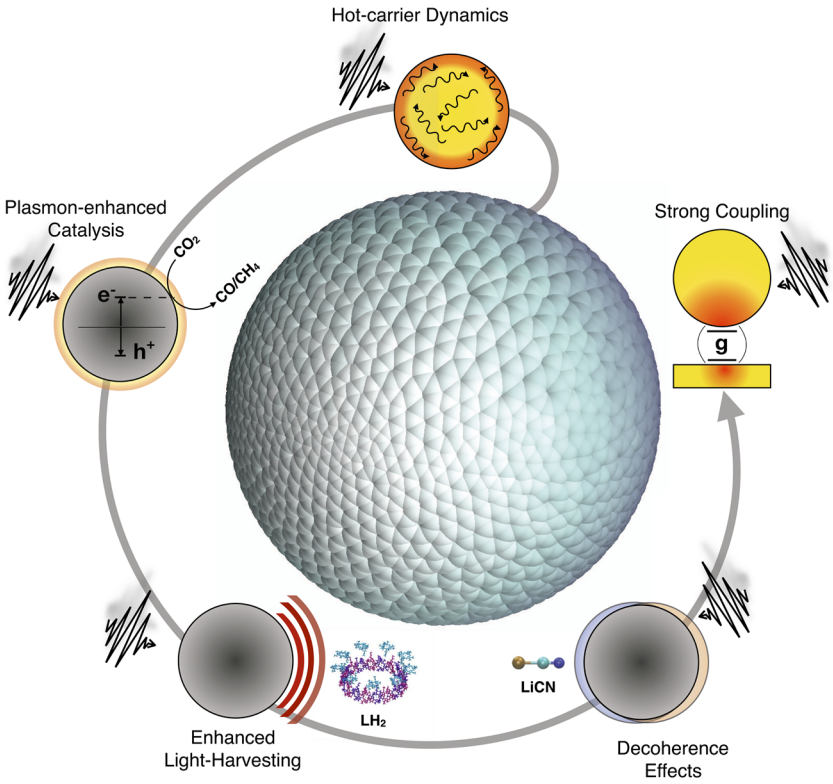

FIG. 1. Graphical summary of the molecular nanoplasmonics topics discussed in this Perspective.

polaritonic chemistry,[47,68–71] and the problem of HC generation and dynamics in NPs and their injection into close molecules,[72–74] as well as the role of HCs in plasmon-enhanced catalytic reactions.[75]

Each topic is discussed starting by a short introduction and overview of the state of the art, followed by a description of the main theoretical approaches applied to the topic, open challenges for QM/continuum models, and possible future developments. In particular, Sec. III A reports on using plasmon-based processes to control excitations in light-harvesting systems and discuss the role of coherence; the molecule–plasmon strong coupling is presented in Sec. III B; the modeling of HC generation, dynamics, and injection into molecules from plasmonic NPs is given in Sec. III C; and how theory and simulations can help in the understanding of the plasmon-enhanced catalysis is shown in Sec. III D. We focus our discussion on QM/continuum models whose basic concepts and relevant recent developments are reviewed in Sec. II.

II. BASIC FEATURES OF QM/CONTINUUM MODELS

In this section, we introduce the main features of QM/continuum models.[11,12,27,36,38–42,45,46] We present their traditional formulation (i.e., in the frequency domain) and then discuss the extension to the time domain. We discuss, in particular, the model that has been dubbed PCM-NP (to underline its conceptual relation with the PCM)[6] whose foundation was laid almost 20 years ago.[36]

A. QM/continuum models: Frequency domain

Within QM/continuum models, the NP is represented as a continuous body characterized by its response properties to electric fields, i.e., the external field and that generated by a neighboring QM charge distribution: a conductor for static perturbations and a dielectric characterized by a frequency-dependent complex permittivity $\epsilon(\omega)$ for time-dependent perturbations. In the quasistatic limit, the electrostatic potential (or field) resulting from the polarization of the NP is the solution of a Poisson equation with proper boundary conditions.[36] The molecular system is instead described at the QM level of theory.

A general approach to simulate the NP response is to define a set of apparent charges (ACs) $\mathbf{q}$ on the surface of the NP, which is discretized in terms of a mesh of elements, called tesserae. This choice ensures an excellent compromise between accuracy and computational cost. No specific limitation due to the NP shape is given. Each tessera is characterized by a representative position and area. The $\mathbf{q}$ charges are described by complex numbers. The AC technique is numerically implemented by using the boundary element method (BEM). The BEM has been successfully employed in the classical description of plasmonic fields originating from general-shaped NPs in the presence of an external field and/or in the proximity of a system treated at a quantum level.[6] In these conditions,

NPs polarize as a response to an external field (external polarization) and to the perturbed quantum mechanical electron density (molecular polarization), providing, in turn, a polarization field to the quantum system.[51] Within such a formulation, the induced charges are written in terms of the total polarizing potential ($\mathbf{V}$), the sum of the external and molecular contributions, and computed at the tesserae position,

$$\mathbf{q}(\omega) = \mathbf{Q}(\omega)\,\mathbf{V}(\omega), \tag{1}$$

where $\mathbf{Q}(\omega)$ is the frequency-dependent response matrix, which depends on the NP surface tesserae (hence, on the NP geometry) and NP dielectric properties.[6] The $\epsilon(\omega)$ function is typically taken by experimental data, possibly corrected for the limited mean free path of electrons in the nanoparticle.[76]

Within the PCM-NP, the continuum model for the NP systems was successfully coupled to HF/TDHF and then to DFT/TDDFT.[11,12,36,77] Linear-response TDDFT[78] provides important information on excited states, such as its decomposition in terms of single-particle transitions. Recently developed algorithms, based on an approximate method to compute the absorption spectrum from the imaginary part of dynamic polarizability,[79,80] allow one to overcome the computational burden when looking at the high-energy part of the spectrum.[81]

B. QM/continuum models: Time domain

In order to provide an accurate and physically meaningful description of the fast and ultrafast phenomena occurring when a NP (or a nanocavity) and a molecular system mutually interact with an external electromagnetic field, a time-resolved approach becomes mandatory (Fig. 2). Focusing on ultrafast electronic processes, a time-domain QM/continuum model has to properly describe the time evolution of the molecular density, via the appropriate formulation of the time-dependent Schrödinger equation, and of the coupled set of ACs, using a classical electromagnetic solver.

A computationally convenient time-resolved version of the BEM has been recently proposed,[53,82] where the set of ACs, now time-dependent [$\mathbf{q}(t)$], can be formally obtained by Fourier transforming Eq. (1),

$$\mathbf{q}(t) = \int_{-\infty}^{+\infty} \mathbf{Q}(t-t')\,\mathbf{V}(t')\mathrm{d}t'. \tag{2}$$

This makes the time-resolved BEM a powerful tool for describing the time evolution of a quantum system interacting with a NP,

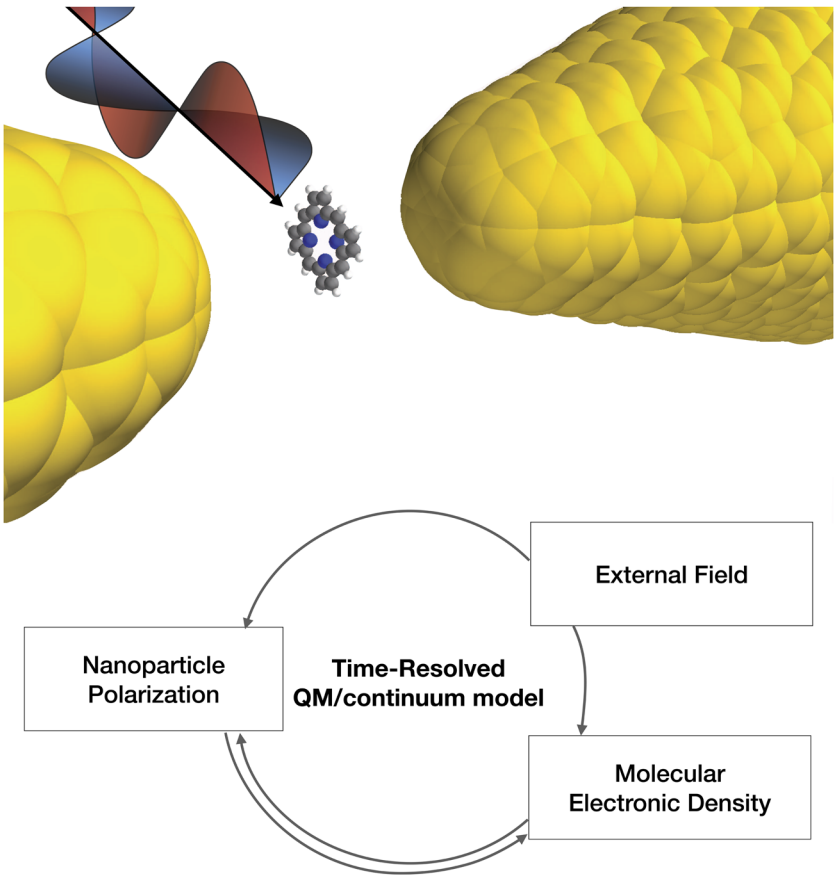

FIG. 2. Scheme representation of a time-resolved QM/continuum model applied to molecular plasmonics.

giving rise to a model that can be dubbed TD-PCM-NP. An alternative approach to the BEM is given by using the finite difference time-domain solver, coupled to real-time TDDFT.[40,42,83,84]

In what follows, we will focus on the quasistatic limit, but it is worth reminding here that the full coupling between a QM molecule and a dielectric (e.g., a NP) within BEM formulations has also been developed.[85]

Within the TD-PCM-NP, the time-dependent Schrödinger equation of the subsystem of interest, $|\Psi_S(t)\rangle$, is propagated using the time-dependent Schrödinger equation,

$$i\frac{d}{dt}|\Psi_S(t)\rangle = \hat{H}_S(t)|\Psi_S(t)\rangle, \tag{3}$$

with

$$\hat{H}_S(t) = \hat{H}_0 - \vec{\hat{\mu}}\cdot\vec{E}_{ext}(t) + \hat{H}_{pol}, \tag{4}$$

where $\hat{H}_0$ is the field-free electronic Hamiltonian, $\vec{\hat{\mu}}$ is the system dipole, and $\hat{H}_{pol}$ is the polarization interaction term, given as

$$\hat{H}_{pol}(t) = \mathbf{q}(t)\cdot\hat{\mathbf{V}}, \tag{5}$$

where $\hat{\mathbf{V}}$ is the generic electrostatic potential operator evaluated at the NP surface representative points. The electrostatic potential, which polarizes the NP, originates from the external field $\vec{E}_{ext}(t)$ and from the molecular density. Examples of $\hat{H}_{pol}$ will be given in Secs. III A and III D for different systems.

The time-dependent system wavefunction $|\Psi_S(t)\rangle$ is expanded using the eigenstate basis $\{|\lambda\rangle\}$ of $\hat{H}_0$,[13,53,86]

$$|\Psi_S(t)\rangle = \sum_\lambda C_\lambda(t)|\lambda\rangle, \tag{6}$$

with λ running over the electronic eigenstates and $C_\lambda(t)$ being time-dependent coefficients evolving according to the Hamiltonian $\hat{H}_S(t)$.

Relaxation (i.e., decay of an electronic excited state to the ground state) and dephasing (i.e., the loss of quantum coherence between the superimposed molecular states) have been recently enclosed in TD-PCM-NP by means of the theory of open quantum systems[87] (Fig. 3). Decoherence of the quantum state can strongly affect the spectroscopic response of the system[13,86,88,89] because the timescales of the relevant physical processes for nanophotonics (from few to hundreds of fs) are those of the typical electronic and vibronic dephasing.[90] Such implementation[13,86] is based on the stochastic formulation of the time-dependent Schrödinger equation (SSE),[91,92] originally developed within the field of quantum optics.[93,94] The SSE implements the physics of open quantum systems using the system wave function, instead of the density matrix used in the master-equation formalism.[95,96] The SSE in the Markovian limit is given by[86,92]

$$i\frac{d}{dt}|\Psi_S(t)\rangle = \hat{H}_S(t)|\Psi_S(t)\rangle + \sum_q^M l_q(t)\hat{S}_q|\Psi_S(t)\rangle - \frac{i}{2}\sum_q^M \hat{S}_q^\dagger\hat{S}_q|\Psi_S(t)\rangle, \tag{7}$$

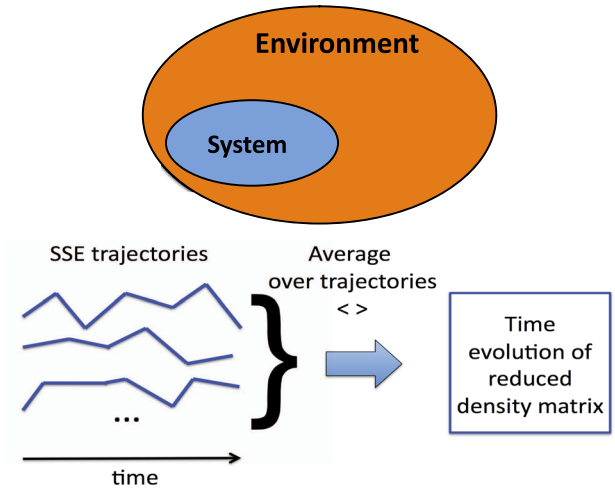

FIG. 3. System and environment separation within the theory of open systems and a schematic representation of a SSE simulation and post-processing.

where $\hat{S}_q$ describes the effect of the environment on the quantum system, through the M interaction channels q. The non-Hermitian term $-\frac{i}{2}\sum_q^M \hat{S}_q^\dagger\hat{S}_q$ describes the dissipation, whereas $\sum_q^M l_q(t)\hat{S}_q$ is the fluctuation, modeled by using a Wiener process $l_q(t)$, both generated by the environment. The system coincides with the degrees of freedom (DOF), which are explicitly treated at the quantum level, as the electronic structure of a molecule, while the environment contains all the other degrees of freedom whose description is encoded in the dissipation and fluctuation terms. In the Markovian limit, the autocorrelation function of the environment is a δ function.[97]

Populations and coherences of the states of the system at time t are extracted from the density matrix, $\hat{\rho}_S(t)$, obtained by averaging on the number of independent SSE realizations,[86] as shown in Fig. 3.

It should be remarked that in the application of the SSE to TD-PCM-NP made so far,[13] the environment responsible for the $\hat{S}_q$ terms is added on top of the dielectric environment (i.e., the NP) whose interaction with the molecule is, instead, treated deterministically following standard TD-PCM-NP. A further step to be accomplished is to move toward a multiscale approach where the NP is properly treated as part of the environment as defined in the theory of open quantum system: the correlation function of the environment will no longer be a δ function (as in the Markovian regime) but will be built from the time-dependent kernel of the non-Markovian SSE in terms of the time-dependent polarization of the NP.[53] Such formal connection has been recently developed in Ref. 98, but not implemented yet.

III. SELECTED MOLECULAR NANOPLASMONICS APPLICATIONS

In this section, we discuss selected topics of current interest in molecular nanoplasmonics that may benefit from the application of QM/continuum models, as anticipated in the Introduction. The order of the topics' presentation reflects the maturity of

QM/continuum models to treat each of them, leaving HC-induced photochemistry and plasmon-assisted catalysis at the end as they require the description of electron exchanges between the molecule and plasmonic nanostructures, which is obviously a challenge when a classical, continuum description is used.

A. Enhanced light-harvesting by nanoplasmonics

A localized surface-plasmon resonance (LSPR) of a NP can intensify light scattering and enhance light concentration around the structure, creating a so-called hot spot.[31,99–102] As a consequence, for instance, the fluorescence of an emitting system placed in such localized hot spots can be greatly increased as a result of the enhancement of the excitation field and of radiative rate modifications, which increases the effective quantum efficiency.[17,100] Moreover, because of the higher radiative rate, the excited-state lifetime is reduced with a resulting increase in photo-stability. Enhancement and quenching of emission (or absorption) of a molecule or a molecular aggregate, due to plasmonic effects by a close NP, is well understood by the coherent sum of the external field effects (exciting both the molecule and the NP) and those arising from the induced field, generated as a response to the external perturbation.[30,31]

It has been experimentally shown that the same strategy applied to organic dyes can also be exploited to enhance light-harvesting (LH) properties of natural photosynthetic systems.[88] In particular, the LH efficiency can be drastically enhanced by tuning the plasmon frequency of the constituent plasmonic particles to the maximal photon flux of sunlight.[103,104] Besides, using plasmonic NPs is a promising way to control excitons in LH complexes;[105] indeed, in supramolecular aggregates, light can be absorbed collectively by many chromophores, giving rise to molecular excitons, i.e., delocalized excited states comprising a superposition of excitations at the different molecular sites. The state coherences are then used to collect light and transfer the excitation energy through space up to the reaction centers, where charge separation occurs.[106] The ability to control excitons in space and time is a priority needed both for our understanding of the natural photosynthetic process at the molecular level and for an optimal development of the exciton-based nanotechnology, which aims to supplant traditional electronics.[89] A quantitative modeling machinery is, therefore, necessary to achieve a complete molecular picture of these processes. The whole absorbing complex is too large to be tackled by a single electronic-structure calculation; hence, a multiscale approach is required.[6,107] In this context, a protocol has been recently developed.[57,58]

- The supramolecular system composed of N_{sites} single chromophores (or equivalent elementary components) is described by an excitonic approximation, where the Hamiltonian

$$\hat{H}_{exc} = \sum_{j}^{N_{sites}} \varepsilon_j |j\rangle\langle j| + \sum_{j\neq k}^{N_{sites}} V_{jk} |j\rangle\langle k| \tag{8}$$

  includes excitation energies (ε_j, usually computed at the QM level) of the single chromophore j, the corresponding localized wave function $|j\rangle$, and the mutual interactions (V_{jk}). This last term is often divided into Coulomb and short-range interactions, with the latter being typically negligible because of the exponential decay with distance. The Coulomb term can be directly calculated from the transition densities.[108,109] Diagonalization of the excitonic Hamiltonian of Eq. (8) provides the excitonic energies and the adiabatic (A) description of the QM system,

$$|\Psi_A\rangle = \sum_j C_j^A |j\rangle. \tag{9}$$

  The excitonic picture can be extended to include charge-transfer (CT) states. To this aim, the chromophoric units describing the CT process (such as a molecular dimer or a trimer) are defined. The excited-state calculation is performed on the basis of such CT units, and a diabatization approach is applied to recover the pure (or diabatic) locally excited and CT states with the corresponding couplings.[110,111] The relative energy of local and CT states is strongly affected by the presence of a polarizable embedding.[107,111–113]
- The electrostatic and polarization effects of the protein scaffold are taken into account by a polarizable embedding scheme.[114] QM/MM methods are the most suited to represent a complex and inhomogenous system as a protein. The most common formulation of QM/MM methods assumes a direct interaction between the QM and the classical parts only through electrostatics, in which the classical atoms are represented as fixed point charges. This electrostatic embedding formulation of QM/MM methods has been extended to include mutual polarization effects, i.e., QM/MMpol between the two subsystems, through an induced dipole formulation. Within this framework, the classical atoms are described as fixed point charges (or fixed multipolar distributions) and characterized by an isotropic static polarizability: each classical particle becomes a polarizable site that responds to the field due to the QM part by generating an atomic-induced dipole that polarizes back the QM part until self-consistency.
- The interactions with the metal NP can be treated by classical electrodynamics and modeled by using a continuum approach, as explained in Sec. II.

This three-layer multiscale approach (QM/MMPol/continuum), involving an atomistic and a continuum model at the same time, has been used to study plasmonic effects on the light-harvesting properties of natural photosynthetic systems, such as the Fenna–Matthews–Olson (FMO) complex[57] and the LH2 complex from photosynthetic purple bacterium Rhodopseudomonas acidophila, in the presence of gold NPs of different shapes, dimensions, and configurations (Fig. 4).[58,59] In both cases, the QM part has been described by using the excitonic method implemented in a TDDFT fashion.[115] In the analyzed FMO-gold NP devices, high fluorescence enhancements were observed for different setups.[57] Enhancements of up to two orders of magnitude were obtained upon irradiation of the intermediate excited states of the protein, which showed stronger absorption enhancements because of their better alignment with the metal aggregates. Orientation effects seem to be crucial: amplifications up to a factor of 300 were observed for the absorption process, while the radiative decay of the emitting state increased, at most, by a factor of

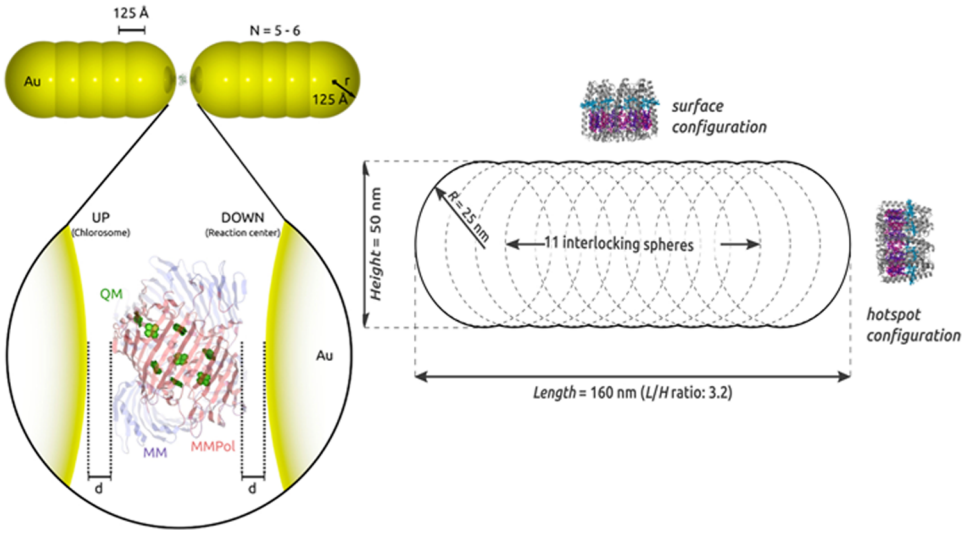

FIG. 4. Schematic representation of the biohybrid systems involving gold nanorods and the natural photosynthetic systems: FMO (left) and LH2 (right). Adapted with permission from Andreussi *et al.*, J. Phys. Chem. A **119**, 5197 (2015) and Caprasecca *et al.*, J. Phys. Chem. Lett. **7**, 2189 (2016). Copyright 2015 and 2016 American Chemical Society.

10, mostly as a result of poor alignment of the emitting state with the considered metal aggregates. As a result, for all the simulated configurations (the number of spheres and aspect ratios), absorption enhancement seems to play the crucial role in determining the overall fluorescence enhancement of the device.

On the same foot, by comparing a hierarchy of models where the excitonic units are modified (from the single bacteriochlorophyll—BChl—to the dimer) and selected couplings are switched on or off, the investigation[58] of the excitonic processes in LH2 in the presence of gold nanorods (NRs) has revealed how excitons interact with plasmons to give the observed dramatic enhancement in fluorescence. Such an enhancement is possible only in hotspot LH2-NR arrangements, and a fundamental role is played by the orientation of LH2 with respect to the NR surface. The results also clearly indicate that even at short LH2-NR distances, the coherent nature of the excitonic states is only slightly perturbed by the NR, and their delocalization length is not significantly affected. Finally, the multiscale description has been used to justify the applicability of the classical dipolar analyses commonly used in the interpretation of the experiments. The obtained results suggested that in a fine-tuning of the coherences, the dimension of the NP should be comparable to that of the LH2 complex. This was exploited in a further study[59] to demonstrate how optimally tuned tip-shaped particles can selectively excite localized regions of typically coherent systems, eventually narrowing down to probing one single pigment. The calculations showed that this can been achieved on both rings of BChls (called B800 and B850, from their absorption spectrum) of LH2. Based on those results, it was suggested that ultrafast experiments can be carried out, where the excitation is consistently prepared on a single chromophore inside the ring, thanks to the nanoplasmonic tip, and the following quantum diffusion is probed by subsequent light pulses. Taking advantage of the distinctive properties of exciton systems (among which long lifetimes and highly efficient energy transfer) and of the ability to selectively control the pigment excitations, in terms of energy or spatial position, the metal aggregate would act as a selector or switch between the energy and charge-transfer pathways.

Theoretical modeling of ultrafast plasmon-assisted spectroscopies on molecules and complex systems, as FMO and LH2, would benefit from the explicit inclusion of electronic/vibrational relaxation and dephasing channels, as mentioned in Sec. II B. A very promising and challenging direction in this research field, indeed, focuses on the study of the possible role of genuine quantum effects in the dynamics of complex systems. The complexity of the systems under investigation called for the expertise of chemists, physicists, and biologists over the last years.[89,116,117] The potential usefulness of the interplay between the coherence time of the molecular system and the intrinsic timescales of nanoplasmons has been remarked recently.[118] Attention is drawn for the detection, use, and application of quantum coherence at the nanoscale, e.g., high-resolution imaging,[119] coherence-tuned plasmon-based polaritons,[119] development of nano-optical coherence theories,[120,121] surface-plasmon enhancement induced by coherence,[122] quantum control of plasmon resonances in nanophotonics, and nanoscale optical coherence sources.[121,123] However, less is known about the role of quantum coherence in molecular plasmonics.[30,31] Some fundamental open questions are as follows: Does the interplay between the (de)coherence and plasmonic effects play a role in ultrafast molecular processes? Does the dephasing induced by a surrounding environment interacting with the molecular system modulate the optical properties affected by plasmons? How the other parameters (geometry, nature, and relative arrangements) affect such an interplay?

While these questions remain open for large systems such as FMO and LH2, a first attempt to answer them is presented in a recent work,[13] using a multiscale *ab initio* approach based on the SSE.[87] A time-domain QM/continuum approach with SSE [Eq. (7)] has been, therefore, recently proposed.[13] As anticipated in Sec. II, the SSE framework can be coupled to the time-resolved formulation of BEM [Eq. (2)] and to electronic-structure methods as DFT/TDDFT

and configuration interaction (CI). The system is defined by the electronic degrees of freedom of the molecule. Time propagation is practically performed through a combination of deterministic dissipative dynamics and quantum jumps.[86,93,94] Interaction channels by means of the $\hat{S}_q$ operators of Eq. (7) imply relaxation (spontaneous emission and nonradiative decay with times T_1) and pure electronic dephasing with time T_2. (De)coherence can control molecular absorption in the presence of a plasmonic NP: in specific conditions, a fast (electronic) dephasing generates a decoherence between external $\vec{E}_{ext}$ and induces $\vec{E}_{ind}$ (on NP) field effects, leading to an absorption recovery for short molecule–NP distances.[13] These effects were studied for a test system given by a LiCN molecule, a spherical silver NP for a radius equal to 5 nm, and a broadband δ pulse polarized tangentially to the NP surface, as a function of the distance R between the molecule and the NP (upper panel of Fig. 5) in Ref. 13. In that work, it was found that electronic decoherence can, even qualitatively (i.e., enhancement vs quenching), alter the plasmon effects on the absorption of the molecule, in a way that may be detected experimentally. In the fully coherent regime, the normalized excitation rate γ_{exc}^{coh} is given by[30,31]

$$\gamma_{exc}^{coh} \equiv \frac{\gamma_{exc}}{\gamma_{exc}^{0}} = \frac{|\vec{n}_\mu \cdot (\vec{E}_{ext} + \vec{E}_{ind})|^2}{|\vec{n}_\mu \cdot \vec{E}_{ext}|^2}, \tag{10}$$

where γ_{exc} and γ_{exc}^{0} are defined as the molecular excitation rate in the presence of NP and for the bare molecule and $\vec{n}_\mu$ is the unit vector pointing in the direction of the transition dipole moment $\vec{\mu}$. The fields can cancel each other,[11,13,16] as in the example presented in the lower panel of Fig. 5. Decoherence of the electronic state of the molecule "decouples" the contributions from $\vec{E}_{\text{ext}}$ and $\vec{E}_{\text{ind}}$, which sum up incoherently regardless of the value of the relative phase,

$$\gamma_{exc}^{inc} \equiv \frac{|\vec{n}_\mu \cdot \vec{E}_{ext}|^2 + |\vec{n}_\mu \cdot \vec{E}_{ind}|^2}{|\vec{n}_\mu \cdot \vec{E}_{ext}|^2}. \tag{11}$$

In the extreme case of fully incoherent regime, only absorption enhancement is possible. In Ref. 13, for a value of T_2 of 50 fs, still a partial coherence was reported [see the lower panel of Fig. 5 (red curve) in the online version]. By decreasing T_2 fs until 5 fs, a further enhancement of molecular absorption is found according to Eq. (11). Moreover, decoherence is more important at shorter distances, at which the mutual interaction between the molecule and the NP is stronger.

The insights provided by the application of the theory of open quantum systems (i.e., SSE) to ultrafast plasmonic spectroscopy will allow one to explore novel scientific routes from both the computational and experimental points of view. Coherence is, indeed, suggested as a further element to be considered in the design of an experimental setup: plasmonic modulation of molecular absorption is strongly modified when a fast dephasing induced acts on the molecular state, possibly breaking the coherent interaction between $\vec{E}_{ext}$ and $\vec{E}_{ind}$.

Furthermore, the application of this computational protocol to the study of the ultrafast dynamics of HCs in the plasmon-enhanced catalysis, described in Secs. III C and III D, will provide novel information on the interplay between plasmon-assisted

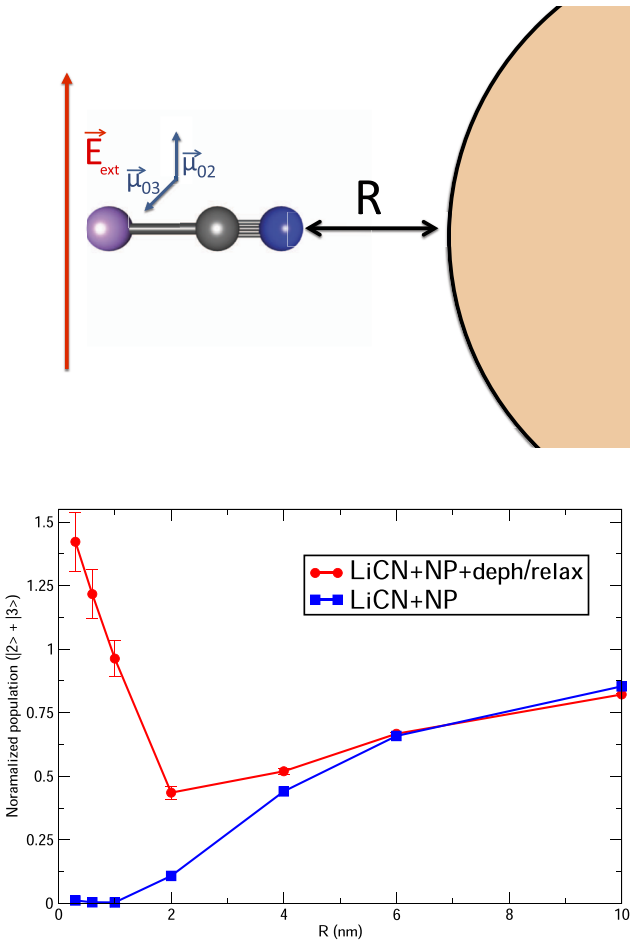

FIG. 5. Upper panel shows the sketch representation of the system studied in Ref. 13. Lower panel shows the decoherence-mediated enhancement of molecular absorption as a function of LiCN–NP distance R. Electron dynamics of 1 ps with T_1 = 1 ps and T_2 = 50 fs, over a range of LiCN–NP distance R between 0.3 nm and 10 nm. Field intensity of 0.1 W/cm^2. Population values are normalized with respect to the respective values without the NP. Reproduced with permission from E. Coccia and S. Corni, J. Chem. Phys. **151**, 044703 (2019). Copyright 2019 AIP Publishing LLC.

generation of HCs and quantum coherence of the state of the system (molecule/molecular fragment + metallic cluster/tip/NP), answering the following open questions: How the efficiency of electron injection will be affected by low or high decoherence regimes? How nonradiative relaxation will modify the fast electron transfer?

Another perspective that deserves to be mentioned is the possible role of plasmon-based mechanisms for high-harmonic generation (HHG) in atomic gases (argon and xenon), which is a source of open debate among experimentalists and theoreticians:[124–127] high-order harmonics could be generated using relatively low-intense pulses (several orders of magnitude lower than the intensities typically applied in HHG experiments), in the presence of irradiated

plasmonic nanotips. If the physical nature of the detected signal is still unclear, with interpretations moving from HHG to multiphoton emission, one could also be interested in studying the role of electronic dephasing on HHG spectra of atoms and molecules,[128] when interacting with plasmonic nanostructures.

B. Quantum coupling between nanoparticles and molecules

The quantum coupling between a metal NP and a neighboring molecule is the interaction occurring between the LSPRs of the NP and molecular transitions. When the molecule and the plasmonic field are confined in a nanometric volume and the system is driven by an external field, the excited plasmonic modes resonate with either the vibrational or the electronic transitions of the molecule. The high intensity of the plasmonic field due to the nanometric confinement allows the NP to exchange energy coherently with the molecule or a portion of it, provided that the molecular transition exhibits a strong transition dipole moment. If such coherent exchange of energy between the molecule and the NP occurs and if it occurs on time scales faster than the decay channels of the system, the system enters the strong-coupling regime. Namely, to achieve this condition, the plasmonic mode and the molecular exciton need to live long enough not to damp the coherent energy exchange. Upon entering the strong-coupling regime, the states of the system are best described as hybrids between light and matter: the polaritons.

While the capability of strong coupling to affect chemistry has first been assessed by coupling many molecules with metal NPs,[68,129] the experimental devising of a setup to achieve single-molecule strong coupling at room temperature is endorsing the idea that single-molecule chemistry can also be tailored by shaping quantum light.

The goal of theoretically describing the dynamical modification of the properties of nanocavities and molecules in the strong coupling is a formidable task. The ideal model should be able to propagate a manifold of quantum modes for the cavity together with the quantum treatment of the molecule, eventually including the external field and the nonradiative events in both the molecule and the NP.[47,130–132] The strong light-molecule Hamiltonian ($\hat{H}_{SC}$) in its general shape consists of three contributions,

$$\hat{H}_{SC} = \hat{H}_{mol} + \hat{H}_{cav} + \hat{H}_{int}. \tag{12}$$

Here, $\hat{H}_{mol}$ is the (model) molecular Hamiltonian described at any level, $\hat{H}_{cav}$ is the quantized electromagnetic field Hamiltonian, and $\hat{H}_{int}$ is the light–matter interaction.

The minimal models to treat the light-molecule strong coupling are borrowed by the modeling of spontaneous emission in confined spaces in quantum optics [Figs. 6(a) and 6(b)]. They consist in taking a two-level quantum emitter as $\hat{H}_{mol}$ [Figs. 6(c) and 6(d)] and couple it via a dipolar transition to a single photon mode, i.e., the Jaynes–Cummings model[133] either including counter rotating terms[134] (Rabi model) or many two-level emitters[135,136] (Dicke and Tavis–Cummings models). Explicitly, the Tavis–Cummings model with N_{emit} emitters provides the following expressions for the terms of Eq. (12):

$$\hat{H}_{mol} = \sum_{n}^{N_{emit}} \omega_n \hat{\sigma}_n^\dagger \hat{\sigma}_n, \tag{13}$$

$$\hat{H}_{cav} = \omega_{cav} \hat{b}^\dagger \hat{b}, \tag{14}$$

$$\hat{H}_{int} = \sum_{n}^{N_{emit}} \left[g_n \left(\hat{\sigma}_n^\dagger \hat{b} + \hat{\sigma}_n \hat{b}^\dagger \right) \right]. \tag{15}$$

Here, ω_n and ω_{cav} are the transition frequencies of the nth emitter and the cavity, $\hat{\sigma}^\dagger$ and σ are the creation and annihilation operators for the molecular excitation of the nth emitter, $\hat{b}^\dagger$ and $\hat{b}$ are the creation and annihilation operators for photon modes, and g_n is the coupling strength between the nth emitter and the quantized light. The coupling term $\hat{H}_{int}$ between each molecular excitation and the quantized light is assumed to be dipolar in the long-wavelength approximation. Hence, a commonly adopted explicit interaction shape makes use of the transition dipole moment of the nth emitter $\hat{\vec{\mu}}^n$ and the single-mode electric field associated with the quantized electromagnetic mode $\vec{E}_{1ph}$ coupled to the molecule, namely,

$$\hat{H}_{int} = \sum_{n}^{N_{emit}} \hat{\vec{\mu}}^n \cdot \vec{E}_{1ph}. \tag{16}$$

$\hat{H}_{int}$ in Eq. (16) coincides with the interaction term of Eq. (4), with the fundamental difference arising from the description of the field, being classical in Eq. (4) and quantum in Eq. (16). Moreover, the $\vec{E}_{1ph}$ term can originate from the external or the NP field. Indeed, the NP–molecule coupling can be computed by the direct quantization of classical plasmonic modes.[137]

Thanks to their simplicity, model Hamiltonians, as the Tavis–Cummings one, are widely exploited and offer a great perspective for a new strong-coupling chemical reactivity,[47,69,138,139] rooting the so-called polaritonic chemistry.[47,140,141] Such approaches based on the model molecules have the great advantage of being able to quickly investigate the polaritonic processes involving a large ensemble of molecules, revealing new effects such as enhanced energy transfer[142–144] or remote control of chemical reactions.[145] However, neglecting the molecular complexity may flatten the rich polariton-assisted chemical reactivity [Figs. 6(e) and 6(f)].[146,147]

The first challenge here is the inclusion of the molecular complexity, e.g., explicitly accounting for the electronic Hamiltonian $\hat{H}_0$ of Eq. (4), for transition dipole moments computed at the QM level and for nuclear motion, as pointed out in Sec. III D. Simulating polaritonic systems is currently being developed by the following two main branches. The first one is to bridge quantum optics with quantum-chemistry methods[148,149] through a reformulation of the traditional quantum-chemistry tools as cavity Born–Oppenheimer[150] or quantum electrodynamics DFT.[151] These quantum-chemistry coupled-to-cavity quantum electrodynamics approaches are mostly advantageous to investigate the modified electronic and vibrational properties of molecules within cavities, yet they sacrifice the realistic description of the experimental setup. The second branch is oriented toward simulating the polaritonic reactivity in realistic environments. This class of methods is based on *ad hoc* developments of the non-adiabatic polaritonic dynamics approaches[146,152] on model molecules. Namely, such

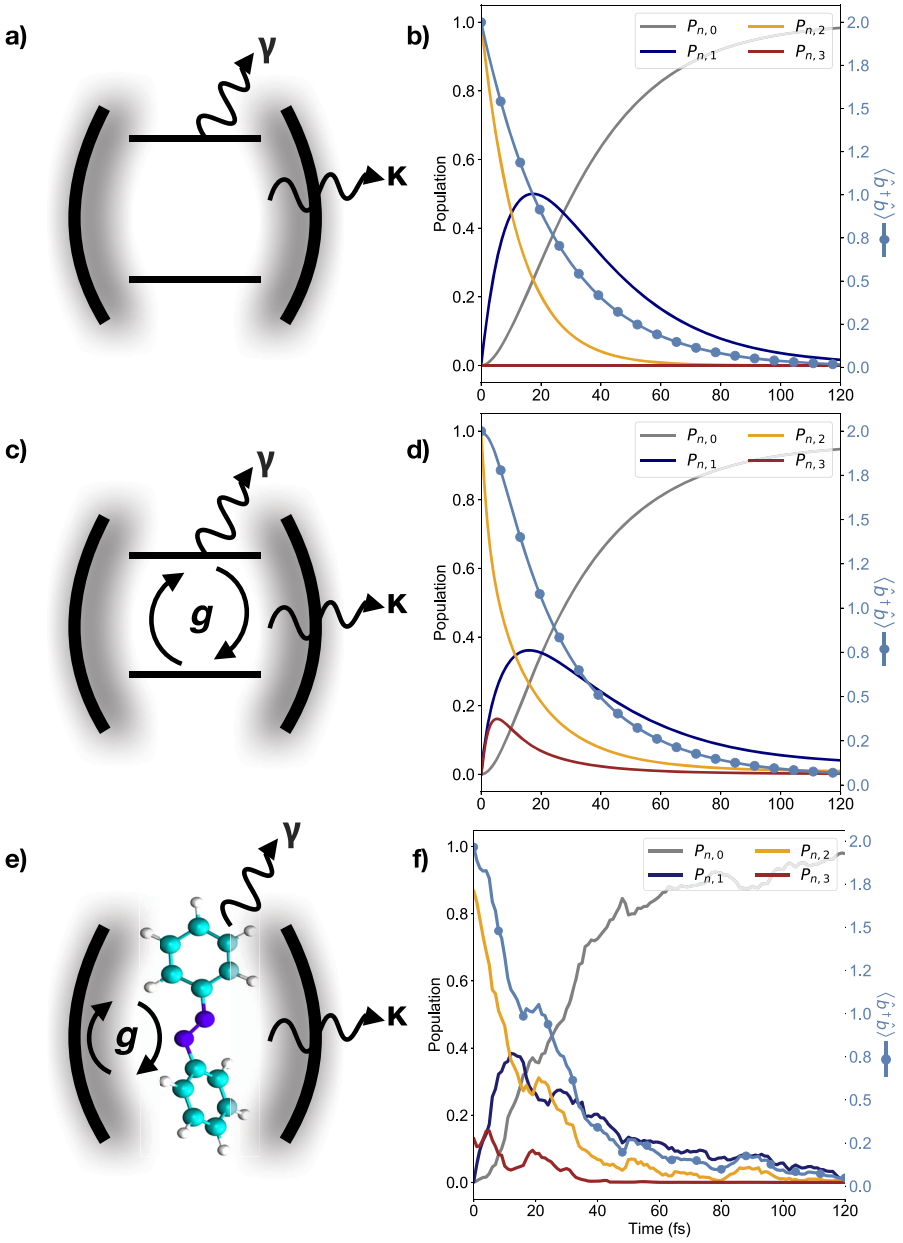

FIG. 6. [(a) and (b)] Population dynamics of a quantum emitter in a cavity starting with photon occupation number $p = 2$—spontaneous emission in the presence of two decay channels κ and γ— namely, the cavity loss and non-radiative decay for the emitter. The dynamics of $p = 2$ in the weak coupling is governed by the dissipative behavior. [(c) and (d)] Quantum Rabi model describing the strong-coupling regime. Several features in the population dynamics arise, such as a non-purely dissipative behavior for $p = 2$, together with a transient population of the $p = 3$ subspace in the first few femtoseconds. [(e) and (f)] Quantum Rabi model for a five-level molecule including non-adiabatic events and nuclear dynamics via surface hopping.[70,71] Together with a transiently increasing total photon number (circled markers), a richer oscillating dynamics is shown as a result of the interplay between the strong-coupling and non-radiative events. The realistic treatment for the molecule also provides on-the-fly information on the molecular structure allowing us to track down the progress of a polaritonic chemical reaction.

methods rely on dressing the electronic states with their interaction with quantized light and, consequently, to simulate the motion of the nuclear wavepacket on the so-obtained polaritonic potential energy surfaces.[70,153,154] The algorithms to simulate the nuclear wavepacket motion are directly borrowed by using the non-adiabatic molecular dynamics techniques, which are largely exploited in simulating photochemical experiments.[155] The benefits of exploiting non-adiabatic techniques are the possibility to treat all the degrees of freedom of a system embedded in an experimentally or biologically relevant environment under strong coupling at both the single- and many-[131,132] molecule level. Some of us recently developed[70] one of these methods based on the direct-trajectories-surface hopping (DTSH) algorithm[156,157] and applied it to the simulation of the polaritonic photochemical isomerization of azobenzene.[71] In the cited work, the electronic structure of the molecule along all the degrees of freedom has been computed by a semi-empirical electronic Hamiltonian[158] (i.e., an *ad hoc* parameterization of $\hat{H}_0$), specifically developed for azobenzene and its derivatives.[159] The QM wave function computed at an approximate CI level[160] is then coupled to a single mode of the electromagnetic field to build the

polaritonic states and the corresponding potential energy surfaces. The motion and splitting of the nuclear wavepacket on the polaritonic potential energy surfaces is treated as a swarm of independent classical trajectories via the DTSH algorithm.[156,161,162] The forces acting on the nuclei are computed analytically at each time step[160,162] by including the force contribution coming from the polaritonic energy. The environment mimics the nanocavity setup experimentally realized by Baumberg and co-workers,[19] and it is included at the QM/MM level with an electrostatic embedding,[157,163,164] while the cavity mode field is taken as a parameter. By the inclusion of all the degrees of freedom, it was shown how chemical and environmental complexities can lead to alternative polaritonic pathways characterized by an enhanced photoisomerization quantum yield for the *trans–cis*-azobenzene isomerization, although only the quenching was predicted on model molecules.[165]

Although the development of methods for strong coupling is rapidly moving to fill the gap between models and experiments, the theoretical description still falls back on several aspects. The size of the optical cavities taken into account limits the description on both the molecular and field components. When tackling microcavities, the huge number of molecular emitters hinders the possibility to accurately describe the chemical complexity of molecules. Careful exploitation of massive parallelization strategies and high performance computing may be a way out to include collective effects.[153]

On the other hand, when nanocavity realizations approach the sub-nanometric field confinement,[166] the possibility to control chemistry on the sub-molecular scale calls for the inclusion of geometrical features arising at both the electromagnetic field and the molecular level. Hybrid models tapping into quantum methods and classical electrodynamics are, indeed, suitable to investigate strong coupling at a sub-nanometric level.[27,137] In particular, in Ref. 27, a QM/continuum model is applied to calculate quantized plasmon-molecule coupling strengths using TDDFT and BEM. It was shown that depending on the molecule, the use of a point dipole approximation may be unsatisfactory, as found before with QM/continuum models for absorption,[36] SERS,[60] and enhanced fluorescence.[12]

Finally, another major open issue is the strong-coupling effect in cavities on the environment embedding the molecule, as a solvent or a more complex chemical scaffold, e.g., proteins or DNA. This is still poorly explored and would require including a quantum character for this component of the system as well.

C. Hot-carrier generation and dynamics

In the process of dephasing and decaying through electron–electron (e–e) scattering, LSPRs efficiently transfer their energy to HCs (electron and holes).[72–74] In the presence of an adsorbate at the metal NP surface or of an interface with a semiconductor, the HCs can eventually be transferred to the adsorbate or to the semiconductor. In this way, the LSPR energy can be exploited in catalysis,[167–169] energy generation,[169] sensing,[170–172] and for plasmon-induced phase transition and doping.[173–175] While the study and use of HCs in the catalysis is the topic of Sec. III D, here, we focus on the description of HC generation and dynamics.

Short timescales and difficulties in controlling the environmental conditions make addressing experimentally these physical processes extremely hard. Theoretical simulations are thus strongly envisaged. However, also on the theoretical side, the accurate description of LSPR-induced HC generation, relaxation, and transfer is extremely challenging. Difficulties arise from dealing with the non-equilibrium excited-state dynamics of an interacting electronic system, possibly coupled to the nuclear degrees of freedom (as pointed out in Sec. III D for the plasmon-enhanced catalysis). Furthermore, the system is intrinsically multiscale both in time and in space: the electronic coupling at the interface requires an atomistic description of that region, whereas the plasmonic NP size ranges from ~10 nm to ~100 nm; the plasmon decays within 10 fs, but HC relaxation and thermalization may take ~100 fs to 1 ps.[176] Theoretical works on this topic provide partial direct and/or indirect information on it, such as HCs' energy and momentum distribution,[74,177–181] population dynamics,[182–185] spectra, lifetime and mean free path,[186,187] plasmon linewidth with respect to adsorbates,[188] and excited-state reaction barriers. In these works, the modeling of the system ranges from jellium[177,179,180] to a full atomistic treatment, and within each model, the interacting electronic system may be treated at different theoretical levels ranging from free-electron models to DFT/TDDFT[189,190] or GW and to the Bethe–Salpeter equation (BSE).[72–74,184,186,191–193]

Real-time implementation of TDDFT has been recently employed to study the mechanism of plasmon-induced HC injection on a prototype metal–acceptor interface ($Ag_{147}Cd_{33}Se_{33}$),[194] at the interface between a TiO_2 slab and an Ag_{20} cluster,[195] and for a CO molecule adsorbed onto Ag_{147}.[196]

In order to further increase the size of the system and to be able to couple a realistic NP to the quantum system of interest, multiscale approaches may be used. QM/continuum models may be directly applicable for a subset of HC experimental systems, i.e., those exploiting the antenna–reactor paradigm,[197] where the plasmonic enhancer (antenna) and the metal cluster providing the HCs (reactor) are physically distinct. For these, the metal cluster is often small[198] and the molecule plus metal cluster may be treated QM, while the antenna may be treated by classical electromagnetic modeling.

When the HCs are generated within the plasmonic system, then the limitations of the QM/continuum (and, in general, QM/classical) models become important. In fact, no electrons are explicitly treated in models such as PCM-NP for the NP component. The grand challenge here is to provide a multiscale model where the NP is treated with an approach computationally affordable (for NPs of tens of nm) yet accurate enough to describe electron or hole transfer to the molecule. Embedding approaches[199] are natural candidates here and have been used already to investigate HC-induced photochemistry.[200–202] The shape and the size of the entire NPs are also important, and the model should be able to include them as well. A combination of quantum mechanical embedding and classical description of the nanoparticle electromagnetic response is a possible line of development here. Such a combination has been achieved at least for the ground state of a molecule on a metal cluster.[203] Pragmatically speaking, an approach that is also worthy to be explored is the use of the molecule as the QM region plus an affordable (a few tens of atoms) portion of the metal NPs, to be coupled with the rest of the NP described classically. While for the ground-state interaction with the molecule, using a sufficiently large cluster may be enough,[204] the question arises whether the optical properties of the

QM+ classical NP are well described. In fact, the QM cluster compared with the corresponding piece of the entire NP suffers by two main artifacts. The first artifact is given by fictitious quantum size effects, related to the confinement of the electronic wavefunctions within the cluster. These effects are appropriate for a real metal cluster, but they should not be there for the model cluster as its electrons are actually delocalized all over the plasmonic NP. The second one is the creation of a time-dependent polarization at the boundary between the QM and the classical part of the NP upon application of an electromagnetic field, which does not exist for the real (whole) NP. How much important these two effects are, which computational strategies can be used to mitigate them, and whether they can be decreased enough to obtain useful calculations are open problems to be investigated. The results obtained by Gao and Neuhauser for a Mg slab treated QM as a whole or partitioned as the QM cluster + classical continuum are encouraging,[42] as well as various reports of a reasonable similarity in local optical properties between fully QM and classical description of tens/hundreds of atoms metal clusters.[49,205,206]

There is a further element to be discussed concerning QM/classical models' applications to HC-induced photochemistry simulations. In this framework, real-time propagation of the electronic wavepacket in the presence of an external electromagnetic field and of a polarizable medium,[6,53] as a NP and/or a solvent, may be obtained solving Eq. (3) or Eq. (7) in conjunction with Eq. (4). Within this methodology, the dynamics of the quantum system has been treated either at the real-time TDDFT level[82] or using the real-time configuration interaction method.[53] DFT and TDDFT for molecules at the interface with solid materials are known to provide inaccurate molecular level vs solid band alignment. As such, while such simulations may be illustrative of the qualitative HC transfer mechanism, they may lack in quantitative accuracy. An accurate alternative to DFT/TDDFT is given by using the GW/BSE approach, developed within the many-body perturbation theory. It provides a correlated description of electronic excitations, giving a picture of the electronic coupling at the molecule/NP interface with a quality higher than that of DFT/TDDFT and comparable to high-level quantum-chemistry methods.[207] At the same time, the GW/BSE approach is more computationally affordable than high-level quantum-chemistry approaches. A further challenge is therefore to extend time-dependent QM/classical models to GW/BSE descriptions.

D. Plasmon-enhanced catalysis

In the last decade, the plasmon-assisted conversion from solar to chemical energy has stimulated great interest in the scientific community.[167,168] Besides the great potential for technological applications,[167] the process has a multiscale (time and size) nature that involves several steps and alternative pathways whose interplay and contribution have not been fully characterized yet.[18,208]

A comprehensive review of what has been experimentally achieved for the plasmon-enhanced catalysis is beyond the scope of this section; hence, only the main features of the recent literature on applications are briefly reported here. Plasmon effects in the catalysis can be of fundamental help to increase the selectivity of desired reaction pathways, to reduce unwanted reaction products, and, in general, to make the reaction faster and more efficient. In order to accomplish that, antenna–reactor complexes have been extensively used.[197,198,209] The idea is to couple (large) NPs with the well-known plasmonic activity (Au, Ag, and Al) with (smaller) transition-metal clusters (Pd, Pt, Fe, Ru, and metal oxides). Transition-metal clusters possess advantageous electronic-structure properties that make them extremely efficient in adsorbing molecules and in triggering surface chemistry. Moreover, they show favorable selectivity[197] compared with thermal processes. The main drawback is their weak interaction with light, preventing transition-metal clusters to improve their (photo)catalytic features. On the other hand, plasmonic metals are characterized by a less intense catalytic activity but support LSPRs with very large optical cross sections. Combining plasmonic and catalytic metal NPs in close proximity to each other, forming a strongly coupled antenna–reactor complex, therefore, becomes a natural and immediate solution to get the best of the two components. Indeed, the combination of plasmonic materials with catalytic metals leads to diversified surface chemistry and reactivity that are not achievable on single-component plasmonic NPs. Alternatively, rhodium NPs exhibit both the plasmonic and photocatalytic features.[210] Water splitting, reduction, and oxidation reactions involving a number of moieties (CO, CO_2, alcohols, aromatic compounds, amines, aldehydes, ketones, alkenes, and alkynes) and polymerization reactions have been widely investigated by means of plasmon-triggered processes.[211,212]

The first step in the plasmon-enhanced catalysis is the generation of HCs (electrons and holes)[4] in the metal arising from the dephasing of the collective charge oscillations of plasmons, as given in Sec. III C. Such HCs can activate chemical reactions involving close molecules, before relaxation mechanisms start taking place (electronic pathway). If such charge transfer is not fast enough, various scattering channels, lowering the HCs' energy, can favor the energy transfer to nuclear vibration (nuclear pathway). Both processes contribute to the determination of the plasmonic enhancement of the reaction rates, yet the factors determining the balance between the two pathways are not clear.[213,214] Hence, future developments in this field are expected to contribute to the clarification of the competition between the electron and nuclear pathways in the plasmon-assisted catalysis. A promising strategy for next developments, based on the multiscale modeling of the steps involved in the process, might focus on (i) the description of the HCs' wave function, (ii) the study of the dynamics of the HCs (iii), and the energy transfer to the nuclear DOF.

Modeling HCs in small metallic nanoparticles (~300 atoms) can be achieved via the TDDFT approach[81] mentioned in Sec. II, but for larger NPs (an average size of 5 nm–25 nm, ~30 000 atoms), a simplified description is necessary. Indeed, free-particle-like approaches have been shown to provide a description of HCs that is in good agreement with DFT, and a first multiscale model combining them with a classical plasmon field has been used to study the HCs' generation in spherical NPs as a function of the size of the NP.[177] Nevertheless, modeling HCs in sizable general-shaped nanoparticles is still a challenge.

Continuum approaches (e.g., BEM) have been successfully applied to the description of free-particle wave functions in general-shaped confining objects.[215] Plasmon-induced generation of HCs can then be simulated within a BEM framework in the

approximation of describing HCs as confined free particles. This approach is fully general and can be applied to both antenna–reactor systems and single NPs: in the former case, the antenna is classically described. In what follows, we, therefore, refer to a generic NP to indicate the plasmonic system generating the HCs. Generally speaking, the BEM approach allows expressing the electric field inside (and outside) the confining NP as generated from auxiliary sources localized on the (discretized) NP surface, Γ, through the electrostatic Green's function. The auxiliary sources are then obtained by solving numerically a set of BEM equations defined by the boundary conditions. The same approach can be applied to free-particle wave functions (ψ_i) because Green's function (G_i) of the Schrödinger equation with zero or a constant potential is known analytically[215] in terms of the energies E_i obtaining

$$\psi_i(\vec{r}) = \int_\Gamma \left[u_i(\vec{s})\partial G_i(\vec{r},\vec{s}) - \partial u_i(\vec{s}) G_i(\vec{r},\vec{s})\right] d\vec{s}. \tag{17}$$

The auxiliary sources u_i and ∂u_i, defined on the boundary mesh, are obtained by solving the BEM equations once the energies E_i have been determined by imposing that BEM equations admit non trivial solutions.[215] Two BEM problems are formulated for ψ_i outside (zero potential) and inside (constant negative potential) the NP. The boundary conditions that define the BEM equations, from Eq. (17) with $\vec{r} \in \Gamma$, are the continuity of the wave function and its derivative on Γ. The value of the (constant) potential inside the NP is defined in order to reproduce the metal work function.[177] BEM equations in this particular case have the form of a linear homogeneous system of equations with size equal to the number of Γ mesh points P. The higher the P, the better the description of high-energy states, but as the computational cost of the best available numerical solution increases as P^3, the solution of the BEM problems for the different states i can be trivially parallelized. The NP, here, is not only intended as a polarizable continuum medium, generating the plasmonic field in its proximity, but also as the confining domain of the HCs that constitute the central quantum system in this multiscale model.

HCs' time evolution is driven primarily by the electron transfer to (from) the absorbed molecule and a fast relaxation (~10 fs–100 fs) dominated by electron–electron (e–e) scattering.[216] Eventually, on longer timescales, the energy can be transferred to vibrations via the electron–phonon coupling.[4] The competition between the fast relaxation and the electron transfer determines the dominant activation pathway. In fact, the e–e scattering, decreasing the energy of HCs, can hamper the electron transfer to/from the molecule, favoring the nuclear activation pathway. One way to address such an issue would be the quantum propagation of the HCs' wave function within the SSE framework.[216] In previous works, HCs' dynamics has been simulated in two steps: first computing the energy distribution in a frequency domain[177] and then evolving the state populations by adding relaxation channels.[216] In this multiscale framework, one could perform a time-domain quantum dynamics, using the set of $|\psi_i\rangle$ as a basis, simulating both the generation and relaxation processes in a single step. The SSE describing the time evolution of all HCs would have the following form:

$$i\frac{d|\Psi_S(t)\rangle}{dt} = \left[\hat{H}_S(t) + \hat{R}\right]|\Psi_S(t)\rangle, \tag{18}$$

where the general form of $\hat{H}_S$ is given by Eq. (4) and $|\Psi_S(t)\rangle$ is the HCs' wave function written as a linear combination of $|\psi_i\rangle$ with time-dependent coefficients. We stress here that being the HCs, the central system $\hat{H}_{pol}$ defines the interaction between the plasmonic field and the HCs, and $\vec{E}_{ext}$ may also contain the time-dependent field generated by the polarized charge density of molecular species adsorbed onto the nanoparticle surface. $\hat{R}$ contains the projectors relative to the different relaxation channels weighted by the respective characteristic rates, namely, according to Eq. (7), $\hat{R} = \sum_q^R l_q(t)\hat{S}_q - \frac{i}{2}\sum_q^R \hat{S}_q^\dagger \hat{S}_q$, with q running over the number R of relaxation channels and $\hat{S}_q$ pure relaxation operators. One could start by only including the e–e relaxation channel because the timescales of the vibrational couplings are at least one order of magnitude longer. In Sec. III A, dephasing channels have also been taken into account. A first estimation of the balance between the nuclear and electron energy pathways would be obtained by comparing the time evolution of the population of HCs at an energy that is higher or equal to the one of the molecular acceptor state, with the electron-transfer rates to molecular states. In fact, only the HCs at energies higher or equal to the molecular acceptor state can be transferred. Transfer rates could be estimated using standard literature approaches (e.g., Marcus theory), with a molecule adsorbed onto a periodic surface or molecule–NP smaller clusters at the DFT level of theory, or similar approaches. We underline that, in principle, the HC injection into molecular empty states could be described by the SSE dynamics, but this would require the computation of mixed integrals between the molecular and HCs' states.

The final step of the process, for both the electronic and nuclear energy pathways, is the energy transfer to the nuclear DOF. Concerning the electronic pathway, the relaxation of the electronic excited (and charged) state of the molecule might be modeled, for simple reactions, via Ehrenfest dynamics[217] of the molecular DOF polarized by the NP described at the classical level.[82]

On the nuclear pathway side, the energy transfer from the NP to the molecule(s) might be modeled via atomistic classical molecular dynamics simulations, allowing the exploration of the plasmon thermal effect on the free-energy barrier of even more complex reactions, including solvent and surface effects, via enhanced sampling techniques. The thermal activation could involve the solvent and molecular species not directly chemisorbed or physisorbed on the NP surface.[218] The energy transfer to vibrations can be simulated via multiple thermostat approaches,[219] and the free-energy barriers can be computed via metadynamics[220] and umbrella sampling.[221] A new topology-based collective variable scheme[222] might be used to describe multi-step, solvent- or surface-assisted reactions where the reaction coordinate is other than trivial. The outcomes of such a multiscale approach would be the setup of the characterization of the competition between the nuclear and electronic energy pathways for a plasmon-assisted catalysis in terms of NP shape, size, and nature and the description of the plasmon effect on free-energy barriers and reaction mechanisms of high-interest chemical reactions including solvent and surface effects. Further developments would concern the inclusion of electron–phonon couplings[223,224] and the description of more complex systems, i.e., adding a semiconductor support or treating coated NPs.[208]

IV. CONCLUSIONS

In this Perspective, we have discussed some of the open challenges in molecular plasmonics that can be theoretically addressed by a combination of different approaches defining efficient and accurate hybrid models. These integrated methods are based on QM/continuum models and coupled to time propagation. Fast and ultrafast dynamics of HCs and nuclei, therefore, become (or will become in the future) accessible to a detailed investigation of the nature of the light–matter interaction at the nanoscale. The outlook reported here covers a selected range of physical phenomena and proposes a direct connection between various areas of the scientific community, from both the theoretical and experimental sides. The development of theoretical models and computational techniques is indeed inspired by a constant dialog with experimental evidences and breakthroughs in nanophotonics, with the final goal of a joint approach for the description, interpretation, and prediction of physical processes of interest.

ACKNOWLEDGMENTS

The authors acknowledge funding from the ERC under Grant No. ERC-CoG-681285 TAME-Plasmons. C.A.G. and S.C. also acknowledge funding from Italian MIUR under Grant No. R164LZWZ4A MIUR-FARE Plasmo-Chem.

DATA AVAILABILITY

Data sharing is not applicable to this article as no new data were created or analyzed in this study.

REFERENCES

[1] K. L. Kelly, E. Coronado, L. L. Zhao, and G. C. Schatz, J. Phys. Chem. B **107**, 668 (2003).
[2] S. M. Morton, D. W. Silverstein, and L. Jensen, Chem. Rev. **111**, 3962 (2011).
[3] S. Kilina, D. Kilin, and S. Tretiak, Chem. Rev. **115**, 5929 (2015).
[4] Y. Zhang, S. He, W. Guo, Y. Hu, J. Huang, J. R. Mulcahy, and W. D. Wei, Chem. Rev. **118**, 2927 (2018).
[5] C. Zhan, X.-J. Chen, J. Yi, J.-F. Li, D.-Y. Wu, and Z.-Q. Tian, Nat. Rev. Chem. **2**, 216 (2018).
[6] B. Mennucci and S. Corni, Nat. Rev. Chem. **3**, 315 (2019).
[7] U. Hohenester, *Nano and Quantum Optics* (Springer Nature Switzerland, 2020).
[8] S. Corni, *Handbook of Molecular Plasmonics: Metal-Molecule Electrodynamic Coupling* (Pan Stanford Publishing, 2013), p. 213.
[9] R. F. Aroca, Phys. Chem. Chem. Phys. **15**, 5355 (2013).
[10] L. Piatkwoswki, N. Accanto, and N. F. van Hulst, ACS Photonics **3**, 1401 (2016).
[11] O. Andreussi, S. Corni, B. Mennucci, and J. Tomasi, J. Chem. Phys. **121**, 10190 (2004).
[12] S. Vukovic, S. Corni, and B. Mennucci, J. Phys. Chem. C **113**, 121 (2009).
[13] E. Coccia and S. Corni, J. Chem. Phys. **151**, 044703 (2019).
[14] S. Schlücker, Angew. Chem., Int. Ed. **53**, 4756 (2014).
[15] A. B. Zrimsek, N. Chiang, M. Mattei, S. Zaleski, M. O. McAnally, C. T. Chapman, A.-I. Henry, G. C. Schatz, and R. P. Van Duyne, Chem. Rev. **117**, 7583 (2017).
[16] E. Dulkeith, M. Ringler, T. A. Klar, J. Feldmann, A. Muñoz Javier, and W. J. Parak, Nano Lett. **5**, 585 (2005).
[17] J. Dong, Z. Zhang, H. Zheng, and M. Sun, Nanophotonics **4**, 472 (2015).
[18] S. Linic, U. Aslam, C. Boerigter, and M. Morabito, Nat. Mater. **14**, 567 (2015).
[19] R. Chikkaraddy, B. de Nijs, F. Benz, S. J. Barrow, O. A. Scherman, E. Rosta, A. Demetriadou, P. Fox, O. Hess, and J. J. Baumberg, Nature **535**, 127 (2016).
[20] M. Ruggenthaler, N. Tancogne-Dejean, J. Flick, H. Appel, and A. Rubio, Nat. Rev. Chem. **2**, 0118 (2018).
[21] L. Jensen, C. M. Aikens, and G. C. Schatz, Chem. Soc. Rev. **37**, 1061 (2008).
[22] A. O. Govorov, Z. Fan, P. Hernandez, J. M. Slocik, and R. R. Naik, Nano Lett. **10**, 1374 (2010).
[23] A. O. Govorov, J. Phys. Chem. C **115**, 7914 (2011).
[24] X. Chen, J. E. Moore, M. Zekarias, and L. Jensen, Nat. Commun. **6**, 8921 (2015).
[25] Z. Hu, D. V. Chulhai, and L. Jensen, J. Chem. Theory Comput. **12**, 5968 (2016).
[26] S. T. Olsen and K. V. Mikkelsen, Phys. Chem. Chem. Phys. **18**, 24343 (2016).
[27] T. Neuman, R. Esteban, D. Casanova, F. J. García-Vidal, and J. Aizpurua, Nano Lett. **18**, 2358 (2018).
[28] A. E. Hillers-Bendtsen, M. H. Hansen, and K. V. Mikkelsen, Phys. Chem. Chem. Phys. **21**, 6689 (2019).
[29] L. Novotny and B. Hecht, *Principles of Nano-Optics* (Cambridge University Press, Cambridge, UK, 2006).
[30] J. Gersten and A. Nitzan, J. Chem. Phys. **75**, 1139 (1981).
[31] P. Anger, P. Bharadwaj, and L. Novotny, Phys. Rev. Lett. **96**, 113002 (2006).
[32] U. Hohenester and A. Trugler, IEEE J. Sel. Top. Quantum Electron. **14**, 1430 (2008).
[33] C. Ciracì and F. Della Sala, Phys. Rev. B **93**, 205405 (2016).
[34] R. Jurga, S. D'Agostino, F. Della Sala, and C. Ciracì, J. Phys. Chem. C **121**, 22361 (2017).
[35] D. J. Masiello, Int. J. Quant. Chem. **114**, 1413 (2014).
[36] S. Corni and J. Tomasi, J. Chem. Phys. **114**, 3739 (2001).
[37] S. M. Morton and L. Jensen, J. Chem. Phys. **133**, 074103 (2010).
[38] K. Lopata and D. Neuhauser, J. Chem. Phys. **130**, 104707 (2009).
[39] K. Lopata and D. Neuhauser, J. Chem. Phys. **131**, 014701 (2009).
[40] H. Chen, J. M. McMahon, M. A. Ratner, and G. C. Schatz, J. Phys. Chem. C **114**, 14384 (2010).
[41] J. Mullin, N. Valley, M. G. Blaber, and G. C. Schatz, J. Phys. Chem. A **116**, 9574 (2012).
[42] Y. Gao and D. Neuhauser, J. Chem. Phys. **138**, 181105 (2013).
[43] Z. Rinkevicius, X. Li, J. A. R. Sandberg, K. V. Mikkelsen, and H. Ågren, J. Chem. Theory Comput. **10**, 989 (2014).
[44] X. Li, Z. Rinkevicius, and H. Ågren, J. Phys. Chem. C **118**, 5833 (2014).
[45] A. Sakko, T. P. Rossi, and R. M. Nieminen, J. Phys. Condens. Matter **26**, 315013 (2014).
[46] Y. Zhang, Z.-C. Dong, and J. Aizpurua, J. Phys. Chem. C **124**, 4674 (2020).
[47] J. Feist, J. Galego, and F. J. Garcia-Vidal, ACS Photonics **5**, 205 (2018).
[48] V. Myroshnychenko, J. Rodríguez-Fernández, I. Pastoriza-Santos, A. M. Funston, C. Novo, P. Mulvaney, L. M. Liz-Marzán, and F. J. García de Abajo, Chem. Soc. Rev. **37**, 1792 (2008).
[49] M. Urbieta, M. Barbry, Y. Zhang, P. Koval, D. Sánchez-Portal, N. Zabala, and J. Aizpurua, ACS Nano **12**, 585 (2018).
[50] J. Marcheselli, D. Chateau, F. Lerouge, P. Baldeck, C. Andraud, S. Parola, S. Baroni, S. Corni, M. Garavelli, and I. Rivalta, J. Chem. Theory Comput. **16**, 3807 (2020).
[51] J. Tomasi, B. Mennucci, and R. Cammi, Chem. Rev. **105**, 2999 (2005).
[52] B. Mennucci, Wiley Interdiscip. Rev.: Comput. Mol. Sci. **2**, 386 (2012).
[53] S. Pipolo and S. Corni, J. Phys. Chem. C **120**, 28774 (2016).
[54] J. L. Payton, S. M. Morton, J. E. Moore, and L. Jensen, Acc. Chem. Res. **47**, 88 (2014).
[55] T. Giovannini, M. Rosa, S. Corni, and C. Cappelli, Nanoscale **11**, 6004 (2019).
[56] L. Bonatti, G. Gil, T. Giovannini, S. Corni, and C. Cappelli, Front. Chem. **8**, 1 (2020).
[57] O. Andreussi, S. Caprasecca, L. Cupellini, I. Guarnetti-Prandi, C. A. Guido, S. Jurinovich, L. Viani, and B. Mennucci, J. Phys. Chem. A **119**, 5197 (2015).

[58]S. Caprasecca, C. A. Guido, and B. Mennucci, J. Phys. Chem. Lett. **7**, 2189 (2016).
[59]S. Caprasecca, S. Corni, and B. Mennucci, Chem. Sci. **9**, 6219 (2018).
[60]S. Corni and J. Tomasi, Chem. Phys. Lett. **342**, 135 (2001).
[61]S. Corni and J. Tomasi, J. Chem. Phys. **116**, 1156 (2002).
[62]M. Caricato, O. Andreussi, and S. Corni, J. Phys. Chem. B **110**, 16652 (2006).
[63]S. Corni and J. Tomasi, "Surface-enhanced Raman scattering: Physics and applications," in *Topics in Applied Physics*, edited by K. Kneipp, M. Moskovits, and H. Kneipp (Springer-Verlag, Berlin, Heidelberg, 2006), Vol. 103, pp. 105–124.
[64]A. Angioni, S. Corni, and B. Mennucci, Phys. Chem. Chem. Phys. **15**, 3294 (2013).
[65]Z. Hu and L. Jensen, J. Chem. Theory Comput. **14**, 5896 (2018).
[66]Y. Zhang, Q. S. Meng, L. Zhang, Y. Luo, Y. J. Yu, B. Yang, Y. Zhang, R. Esteban, J. Aizpurua, Y. Luo, J. L. Yang, Z. C. Dong, and J. G. Hou, Nat. Commun. **8**, 15225 (2017).
[67]J. T. Hugall, A. Singh, and N. F. van Hulst, ACS Photonics **5**, 43 (2018).
[68]J. A. Hutchison, T. Schwartz, C. Genet, E. Devaux, and T. W. Ebbesen, Angew. Chem., Int. Ed. **51**, 1592 (2012).
[69]F. Herrera and F. C. Spano, Phys. Rev. Lett. **116**, 238301 (2016).
[70]J. Fregoni, G. Granucci, E. Coccia, M. Persico, and S. Corni, Nat. Commun. **9**, 4688 (2018).
[71]J. Fregoni, G. Granucci, M. Persico, and S. Corni, Chem **6**, 250 (2020).
[72]M. Bernardi, J. Mustafa, J. B. Neaton, and S. G. Louie, Nat. Commun. **6**, 7044 (2015).
[73]A. M. Brown, R. Sundararaman, P. Narang, W. A. Goddard, and H. A. Atwater, ACS Nano **10**, 957 (2016).
[74]R. Sundararaman, P. Narang, A. S. Jermyn, W. A. Goddard III, and H. A. Atwater, Nat. Commun. **5**, 5788 (2014).
[75]L. Zhou, C. Zhang, M. J. McClain, A. Manjavacas, C. M. Krauter, S. Tian, F. Berg, H. O. Everitt, E. A. Carter, P. Nordlander, and N. J. Halas, Nano Lett. **16**, 1478 (2016).
[76]U. Kreibig and C. v. Fragstein, Z. Phys. A **224**, 307 (1969).
[77]O. Andreussi, A. Biancardi, S. Corni, and B. Mennucci, Nano Lett. **13**, 4475 (2013).
[78]M. Casida, *Recent Advances in Density Functional Methods, Part I* (World Scientific, Singapore, 1995).
[79]O. Baseggio, G. Fronzoni, and M. Stener, J. Chem. Phys. **143**, 024106 (2015).
[80]O. Baseggio, M. De Vetta, G. Fronzoni, M. Stener, and A. Fortunelli, Int. J. Quant. Chem. **116**, 1603 (2016).
[81]O. Baseggio, M. De Vetta, G. Fronzoni, M. Stener, L. Sementa, A. Fortunelli, and A. Calzolari, J. Phys. Chem. C **120**, 12773 (2016).
[82]S. Corni, S. Pipolo, and R. Cammi, J. Phys. Chem. A **119**, 5405 (2014).
[83]A. Sakko, T. P. Rossi, J. Enkovaara, and R. M. Nieminen, Appl. Phys. A **115**, 427 (2013).
[84]H. T. Smith, T. E. Karam, L. H. Haber, and K. Lopata, J. Phys. Chem. C **121**, 16932 (2017).
[85]S. Pipolo, S. Corni, and R. Cammi, J. Chem. Phys. **140**, 164114 (2014).
[86]E. Coccia, F. Troiani, and S. Corni, J. Chem. Phys. **148**, 204112 (2018).
[87]H.-P. Breuer and F. Petruccione, *The Theory of Open Quantum Systems* (Oxford University Press, Oxford, 2006).
[88]E. Wientjes, J. Renger, A. G. Curto, R. Cogdell, and N. F. van Hulst, Nat. Commun. **5**, 4236 (2014).
[89]G. D. Scholes, G. R. Fleming, L. X. Chen, A. Aspuru-Guzik, A. Buchleitner, D. F. Coker, G. S. Engel, R. van Grondelle, A. Ishizaki, D. M. Jonas, J. S. Lundeen, J. K. McCusker, S. Mukamel, J. P. Ogilvie, A. Olaya-Castro, M. A. Ratner, F. C. Spano, K. B. Whaley, and X. Zhu, Nature **543**, 647 (2017).
[90]D. Brinks, R. Hildner, E. M. H. P. van Dijk, F. D. Stefani, J. B. Nieder, J. Hernando, and N. F. van Hulst, Chem. Soc. Rev. **43**, 2476 (2014).
[91]R. Biele and R. D'Agosta, J. Phys. Condens. Matter **24**, 273201 (2012).
[92]A. J. Daley, Adv. Phys. **63**, 77 (2014).
[93]J. Dalibard, Y. Castin, and K. Mølmer, Phys. Rev. Lett. **68**, 580 (1992).
[94]K. Mølmer, Y. Castin, and J. Dalibard, J. Opt. Soc. Am. B **10**, 524 (1993).
[95]E. Palacino-González, M. F. Gelin, and W. Domcke, Phys. Chem. Chem. Phys. **19**, 32296 (2017).
[96]E. Palacino-González, M. F. Gelin, and W. Domcke, Phys. Chem. Chem. Phys. **19**, 32307 (2017).
[97]P. Gaspard and M. Nagaoka, J. Chem. Phys. **111**, 5676 (1999).
[98]C. A. Guido, M. Rosa, R. Cammi, and S. Corni, J. Chem. Phys. **152**, 174114 (2020).
[99]K. A. Willets and R. P. Van Duyne, Annu. Rev. Phys. Chem. **58**, 267 (2007).
[100]T. Ming, H. Chen, R. Jiang, Q. Li, and J. Wang, J. Phys. Chem. Lett. **3**, 191 (2012).
[101]F. J. García de Abajo, ACS Photonics **1**, 135 (2014).
[102]K. Saha, S. S. Agasti, C. Kim, X. Li, and V. M. Rotello, Chem. Rev. **112**, 2739 (2012).
[103]S. Mackowski, S. Wörmke, A. J. Maier, T. H. P. Brotosudarmo, H. Harutyunyan, A. Hartschuh, A. O. Govorov, H. Scheer, and C. Bräuchle, Nano Lett. **8**, 558 (2008).
[104]I. Carmeli, I. Lieberman, L. Kraversky, Z. Fan, A. O. Govorov, G. Markovich, and S. Richter, Nano Lett. **10**, 2069 (2010).
[105]I. Carmeli, M. Cohen, O. Heifler, Y. Lilach, Z. Zalevsky, V. Mujica, and S. Richter, Nat. Commun. **6**, 7334 (2015).
[106]G. D. Scholes and G. Rumbles, Nat. Mater. **5**, 683 (2006).
[107]C. A. Guido and S. Caprasecca, Int. J. Quantum Chem. **119**, e25711 (2019).
[108]M. F. Iozzi, B. Mennucci, J. Tomasi, and R. Cammi, J. Chem. Phys. **120**, 7029 (2004).
[109]C.-P. Hsu, G. R. Fleming, M. Head-Gordon, and T. Head-Gordon, J. Chem. Phys. **114**, 3065 (2001).
[110]L. Cupellini, S. Jurinovich, M. Campetella, S. Caprasecca, C. A. Guido, S. M. Kelly, A. T. Gardiner, R. Cogdell, and B. Mennucci, J. Phys. Chem. B **120**, 11348 (2016).
[111]L. Cupellini, S. Caprasecca, C. A. Guido, F. Müh, T. Renger, and B. Mennucci, J. Phys. Chem. Lett. **9**, 6892 (2018).
[112]C. A. Guido, D. Jacquemin, C. Adamo, and B. Mennucci, J. Chem. Theory Comput. **11**, 5782 (2015).
[113]C. A. Guido, G. Scalmani, B. Mennucci, and D. Jacquemin, J. Chem. Phys. **146**, 204106 (2017).
[114]C. Curutchet, A. Muñoz-Losa, S. Monti, J. Kongsted, G. D. Scholes, and B. Mennucci, J. Chem. Theory Comput. **5**, 1838 (2009).
[115]S. Jurinovich, L. Cupellini, C. A. Guido, and B. Mennucci, J. Comput. Chem. **39**, 279 (2018).
[116]G. D. Scholes, J. Phys. Chem. Lett. **1**, 2 (2010).
[117]E. Collini, Chem. Soc. Rev. **42**, 4932 (2013).
[118]S. I. Bogdanov, A. Boltasseva, and V. M. Shalaev, Nature **364**, 532 (2019).
[119]D. Morrill, D. Li, and D. Pacifici, Nat. Photonics **10**, 681 (2016).
[120]A. Cazé, R. Pierrat, and R. Carminati, Phys. Rev. Lett. **110**, 063903 (2013).
[121]K. E. Dorfman, P. K. Jha, D. V. Voronine, P. Genevet, F. Capasso, and M. O. Scully, Phys. Rev. Lett. **111**, 043601 (2013).
[122]R. U. Din, X.-D. Zeng, G.-Q. Ge, and M. S. Zubairy, Opt. Express **27**, 322 (2019).
[123]P. K. Jha, X. Yin, and X. Zhang, Appl. Phys. Lett. **102**, 091111 (2013).
[124]S. Kim, J. Jin, Y.-J. Kim, I.-Y. Park, Y. Kim, and S.-W. Kim, Nature **453**, 757 (2008).
[125]M. Sivis, M. Duwe, B. Abel, and C. Ropers, Nature **485**, E1 (2012).
[126]M. B. Raschke, Ann. Phys. **525**, A40 (2013).
[127]M. Blanco, C. Hernández-García, A. Chacón, M. Lewenstein, M. T. Flores-Arias, and L. Plaja, Opt. Express **25**, 14974 (2017).
[128]E. Coccia, "How electronic dephasing affects the high-harmonic generation in atoms," Mol. Phys. **118**(23), e1769871 (2020).
[129]T. Schwartz, J. A. Hutchison, C. Genet, and T. W. Ebbesen, Phys. Rev. Lett. **106**, 196405 (2011).
[130]A. Delga, J. Feist, J. Bravo-Abad, and F. J. Garcia-Vidal, Phys. Rev. Lett. **112**, 253601 (2014).
[131]G. Groenhof and J. J. Toppari, J. Phys. Chem. Lett. **9**, 4848 (2018).

[132]G. Groenhof, C. Climent, J. Feist, D. Morozov, and J. J. Toppari, J. Phys. Chem. Lett. **10**, 5476 (2019).
[133]E. T. Jaynes and F. W. Cummings, Proc. IEEE **51**, 89 (1963).
[134]I. I. Rabi, Phys. Rev. **49**, 324 (1936).
[135]R. H. Dicke, Phys. Rev. **93**, 99 (1954).
[136]M. Tavis and F. W. Cummings, Phys. Rev. **170**, 379 (1968).
[137]B. Doppagne, T. Neuman, R. Soria-Martinez, L. E. P. López, H. Bulou, M. Romeo, S. Berciaud, F. Scheurer, J. Aizpurua, and G. Schull, Nat. Nanotechnol. **15**, 207 (2020).
[138]K. Bennett, M. Kowalewski, and S. Mukamel, Faraday Discuss. **194**, 259 (2016).
[139]M. Kowalewski, K. Bennett, and S. Mukamel, J. Chem. Phys. **144**, 054309 (2016).
[140]R. F. Ribeiro, L. A. Martínez-Martínez, M. Du, J. Campos-Gonzalez-Angulo, and J. Yuen-Zhou, Chem. Sci. **9**, 6325 (2018).
[141]J. Yuen-Zhou and V. M. Menon, Proc. Natl. Acad. Sci. U. S. A. **116**, 5214 (2019).
[142]X. Zhong, T. Chervy, L. Zhang, A. Thomas, J. George, C. Genet, J. A. Hutchison, and T. W. Ebbesen, Angew. Chem., Int. Ed. **129**, 9162 (2017).
[143]J. Schachenmayer, C. Genes, E. Tignone, and G. Pupillo, Phys. Rev. Lett. **114**, 196403 (2015).
[144]R. Sáez-Blázquez, J. Feist, A. I. Fernández-Domínguez, and F. J. García-Vidal, Phys. Rev. B **97**, 241407 (2018).
[145]M. Du, R. F. Ribeiro, and J. Yuen-Zhou, Chem **5**, 1167 (2019).
[146]J. Galego, F. J. Garcia-Vidal, and J. Feist, Phys. Rev. X **5**, 041022 (2015).
[147]T. P. Rossi, T. Shegai, P. Erhart, and T. J. Antosiewicz, Nat. Commun. **10**, 3336 (2019).
[148]C. Schäfer, M. Ruggenthaler, and A. Rubio, Phys. Rev. A **98**, 043801 (2018).
[149]J. Flick, C. Schäfer, M. Ruggenthaler, H. Appel, and A. Rubio, ACS Photonics **5**, 992 (2018).
[150]J. Flick, H. Appel, M. Ruggenthaler, and A. Rubio, J. Chem. Theory Comput. **13**, 1616 (2017).
[151]M. Ruggenthaler, J. Flick, C. Pellegrini, H. Appel, I. V. Tokatly, and A. Rubio, Phys. Rev. A **90**, 012508 (2014).
[152]M. Kowalewski, K. Bennett, and S. Mukamel, J. Phys. Chem. Lett. **7**, 2050 (2016).
[153]H. L. Luk, J. Feist, J. J. Toppari, and G. Groenhof, J. Chem. Theory Comput. **13**, 4324 (2017).
[154]I. S. Ulusoy, J. A. Gomez, and O. Vendrell, J. Phys. Chem. A **123**, 8832 (2019).
[155]M. Persico and G. Granucci, Theor. Chem. Acc. **133**, 1526 (2014).
[156]G. Granucci and M. Persico, Theor. Chem. Acc. **117**, 1131 (2007).
[157]A. Toniolo, C. Ciminelli, G. Granucci, T. Laino, and M. Persico, Theor. Chem. Acc. **111**, 270 (2004).
[158]T. Cusati, G. Granucci, E. Martínez-Núñez, F. Martini, M. Persico, and S. Vázquez, J. Phys. Chem. A **116**, 98 (2012).
[159]C. Ciminelli, G. Granucci, and M. Persico, Chem. - Eur. J. **10**, 2327 (2004).
[160]G. Granucci and A. Toniolo, Chem. Phys. Lett. **325**, 79 (2000).
[161]G. Granucci, M. Persico, and A. Zoccante, J. Chem. Phys. **133**, 134111 (2010).
[162]G. Granucci and M. Persico, J. Comput. Chem. **32**, 2690 (2011).
[163]M. Persico, G. Granucci, S. Inglese, T. Laino, and A. Toniolo, J. Mol. Struct.: THEOCHEM **621**, 119 (2003).
[164]A. Toniolo, G. Granucci, and T. J. Martínez, J. Phys. Chem. A **107**, 3822 (2003).
[165]J. Galego, F. J. Garcia-Vidal, and J. Feist, Nat. Commun. **7**, 13841 (2016).
[166]O. S. Ojambati, R. Chikkaraddy, W. D. Deacon, M. Horton, D. Kos, V. A. Turek, U. F. Keyser, and J. J. Baumberg, Nat. Commun. **10**, 1049 (2019).
[167]S. Linic, P. Christopher, and D. B. Ingram, Nat. Mater. **10**, 911 (2011).
[168]P. Christopher, H. Xin, and S. Linic, Nat. Chem. **3**, 467 (2011).
[169]H. Harutyunyan, F. Suchanek, R. Lemasters, and J. J. Foley, MRS Bull. **45**, 32–36 (2020).
[170]J. N. Anker, W. P. Hall, O. Lyandres, N. C. Shah, J. Zhao, and R. P. Van Duyne, Nat. Mater. **7**, 442 (2008).
[171]W. Li, Z. J. Coppens, L. V. Besteiro, W. Wang, A. O. Govorov, and J. Valentine, Nat. Commun. **6**, 8379 (2015).
[172]W. Li and J. Valentine, Nano Lett. **14**, 3510 (2014).
[173]Z. Fang, Y. Wang, Z. Liu, A. Schlather, P. M. Ajayan, F. H. L. Koppens, P. Nordlander, and N. J. Halas, ACS Nano **6**, 10222 (2012).
[174]K. Appavoo, B. Wang, N. F. Brady, M. Seo, J. Nag, R. P. Prasankumar, D. J. Hilton, S. T. Pantelides, and R. F. Haglund, Nano Lett. **14**, 1127 (2014).
[175]A. Hoggard, L.-Y. Wang, L. Ma, Y. Fang, G. You, J. Olson, Z. Liu, W.-S. Chang, P. M. Ajayan, and S. Link, ACS Nano **7**, 11209 (2013).
[176]A. S. Jermyn, G. Tagliabue, H. A. Atwater, W. A. Goddard, P. Narang, and R. Sundararaman, Phys. Rev. Mater. **3**, 075201 (2019).
[177]A. Manjavacas, J. G. Liu, V. Kulkarni, and P. Nordlander, ACS Nano **8**, 7630 (2014).
[178]A. O. Govorov, H. Zhang, and Y. K. Gun'ko, J. Phys. Chem. C **117**, 16616 (2013).
[179]H. Zhang and A. O. Govorov, J. Phys. Chem. C **118**, 7606 (2014).
[180]C. S. Kumarasinghe, M. Premaratne, Q. Bao, and G. P. Agrawal, Sci. Rep. **5**, 12140 (2015).
[181]G. V. Naik and J. A. Dionne, Appl. Phys. Lett. **107**, 133902 (2015).
[182]J. G. Liu, H. Zhang, S. Link, and P. Nordlander, ACS Photonics **5**, 2584 (2018).
[183]J. R. M. Saavedra, A. Asenjo-Garcia, and F. J. García de Abajo, ACS Photonics **3**, 1637 (2016).
[184]A. Crai, A. Pusch, D. E. Reiter, L. Román Castellanos, T. Kuhn, and O. Hess, Phys. Rev. B **98**, 165411 (2018).
[185]O. A. Douglas-Gallardo, M. Berdakin, T. Frauenheim, and C. G. Sánchez, Nanoscale **11**, 8604 (2019).
[186]M. Quijada, R. Díez Muiño, A. G. Borisov, J. A. Alonso, and P. M. Echenique, New J. Phys. **12**, 053023 (2010).
[187]X. Zubizarreta, E. V. Chulkov, I. P. Chernov, A. S. Vasenko, I. Aldazabal, and V. M. Silkin, Phys. Rev. B **95**, 235405 (2017).
[188]B. Foerster, V. A. Spata, E. A. Carter, C. Sönnichsen, and S. Link, Sci. Adv. **5**, eaav0704 (2019).
[189]P. Song, P. Nordlander, and S. Gao, J. Chem. Phys. **134**, 074701 (2011).
[190]V. Kulkarni and A. Manjavacas, ACS Photonics **2**, 987 (2015).
[191]G. Onida, L. Reining, and A. Rubio, Rev. Mod. Phys. **74**, 601 (2002).
[192]A. M. Brown, R. Sundararaman, P. Narang, A. M. Schwartzberg, W. A. Goddard, and H. A. Atwater, Phys. Rev. Lett. **118**, 087401 (2017).
[193]A. Habib, F. Florio, and R. Sundararaman, J. Opt. **20**, 064001 (2018).
[194]P. V. Kumar, T. P. Rossi, D. Marti-Dafcik, D. Reichmuth, M. Kuisma, P. Erhart, M. J. Puska, and D. J. Norris, ACS Nano **13**, 3188 (2019).
[195]J. Ma and S. Gao, ACS Nano **13**, 13658 (2019).
[196]P. V. Kumar, T. P. Rossi, M. Kuisma, P. Erhart, and D. J. Norris, Faraday Discuss. **214**, 189 (2019).
[197]D. F. Swearer, H. Zhao, L. Zhou, C. Zhang, H. Robatjazi, J. M. P. Martirez, C. M. Krauter, S. Yazdi, M. J. McClain, E. Ringe, E. A. Carter, P. Nordlander, and N. J. Halas, Proc. Natl. Acad. Sci. U. S. A. **113**, 8916 (2016).
[198]D. F. Swearer, R. K. Leary, R. Newell, S. Yazdi, H. Robatjazi, Y. Zhang, D. Renard, P. Nordlander, P. A. Midgley, N. J. Halas, and E. Ringe, ACS Nano **11**, 10281 (2017).
[199]F. Libisch, C. Huang, and E. A. Carter, Acc. Chem. Res. **47**, 2768 (2014).
[200]V. A. Spata and E. A. Carter, ACS Nano **12**, 3512 (2018).
[201]J. L. Bao and E. A. Carter, J. Am. Chem. Soc. **141**, 13320 (2019).
[202]J. L. Bao and E. A. Carter, ACS Nano **13**, 9944 (2019).
[203]P. P. Pal, P. Liu, and L. Jensen, J. Chem. Theory Comput. **15**, 6588 (2019).
[204]E. Fabiano, M. Piacenza, S. D'Agostino, and F. Della Sala, J. Chem. Phys. **131**, 234101 (2009).
[205]A. Muñoz-Losa, S. Vukovic, S. Corni, and B. Mennucci, J. Phys. Chem. C **113**, 16364 (2009).
[206]R. Sinha-Roy, P. García-González, H.-C. Weissker, F. Rabilloud, and A. I. Fernández-Domínguez, ACS Photonics **4**, 1484 (2017).
[207]D. Jacquemin, I. Duchemin, and X. Blase, J. Chem. Theory Comput. **11**, 3290 (2015).

[208]G. V. Hartland, Chem. Rev. **111**, 3858 (2011).
[209]D. F. Swearer, H. Robatjazi, J. M. P. Martirez, M. Zhang, L. Zhou, E. A. Carter, P. Nordlander, and N. J. Halas, ACS Nano **13**, 8076 (2019).
[210]X. Zhang, X. Li, D. Zhang, N. Su, W. Yang, and H. Everitt, Nat. Commun. **8**, 14542 (2017).
[211]W. Hou and S. B. Cronin, Adv. Funct. Mater. **23**, 1612 (2013).
[212]A. Gellé, T. Jin, L. de la Garza, G. D. Price, L. V. Besteiro, and A. Moores, Chem. Rev. **120**, 986 (2020).
[213]X. Zhang, X. Li, M. E. Reish, D. Zhang, N. Q. Su, Y. Gutiérrez, F. Moreno, W. Yang, H. O. Everitt, and J. Liu, Nano Lett. **18**, 1714 (2018).
[214]Y. Yu, V. Sundaresan, and K. A. Willets, J. Phys. Chem. C **122**, 5040 (2018).
[215]I. Kosztin and K. Schulten, Int. J. Mod. Phys. C **08**, 293 (1997).
[216]J. Liu, H. Zhang, S. Link, and P. Nordlander, ACS Photonics **5**, 2584 (2018).
[217]L. Yan, J. Xu, F. Wang, and S. Meng, J. Phys. Chem. Lett. **9**, 63 (2017).
[218]J. Guo, Y. Zhang, L. Shi, Y. Zhu, M. F. Mideksa, K. Hou, W. Zhao, D. Wang, M. Zhao, X. Zhang *et al.*, J. Am. Chem. Soc. **139**, 17964 (2017).
[219]X. Chen, A. Munjiza, K. Zhang, and D. Wen, J. Phys. Chem. C **118**, 1285 (2014).
[220]A. Laio and M. Parrinello, Proc. Natl. Acad. Sci. U. S. A. **99**, 12562 (2002).
[221]G. M. Torrie and J. P. Valleau, J. Comput. Phys. **23**, 187 (1977).
[222]S. Pipolo, M. Salanne, G. Ferlat, S. Klotz, A. M. Saitta, and F. Pietrucci, Phys. Rev. Lett. **119**, 245701 (2017).
[223]A. J. Neukirch, Z. Guo, and O. V. Prezhdo, J. Phys. Chem. C **116**, 15034 (2012).
[224]P. V. Kumar and D. J. Norris, ACS Catal. **7**, 8343 (2017).